Analysis of Benchmark Lattices with ENDF/B-VI, JEF-2.2 and JENDL-3 Data

Referans Örgülerin ENDF/B-VI, JEF-2.2 Ve JENDL-3 Verileri Ile Analizi

Mehmet Sağlam

Submitted in partial fullfillment of the requirements for the degree of master of science in the field of nuclear engineering

Hacettepe University
July 1995

To the Institute for Graduate Studies in Pure and Applied Sciences,

This work has been approved by the Graduate Committee as partial fulfillment of the requirements for the degree of MASTER OF SCIENCE in the field of NUCLEAR ENGINEERING.

Graduate Commitee

Head : _____
Doç. Dr. Cemal Niyazi Sökmen

Member : _____
Doç. Dr. Mehmet Tombakoğlu

Member : _____
Prof. Dr. Osman Kemal Kadiroğlu

APPROVED

This thesis has been approved on / / 1995 by the Graduate Commitee established by the Board of the Institute.

28. /8/1995

Prof. Dr. Gültekin GÜNAY
HEAD OF THE INSTITUTE FOR GRADUATE STUDIES IN PURE AND APPLIED SCIENCES

Abstract

The NJOY Nuclear Data Processing System has been used to process the ENDF/B-VI , JEF-2.2 and JENDL-3 Nuclear Cross Section Data Bases into multigroup form. A brief description of the data bases is given and the assumptions made in processing the data from evaluated nuclear data file format to multigroup format are presented. The differences and similarities of the Evaluated Nuclear Data Files have been investigated by producing four group cross sections by using the GROUPIE code and calculating thermal, fission spectrum averaged and 2200 m/s cross sections and resonance integrals using the INTER code. It has been shown that the evaluated data for U^{238} in JEF and ENDF/B-VI are principally the same while in case of U^{235} the same is true for JENDL and ENDF/B-VI. The evaluations for U^{233} and Th^{232} are different for all three ENDF files.

Several utility codes have been written to convert the multigroup library into a WIMS-D4 compatible binary library. The performance and suitability of the generated libraries have been tested with the use of metal fueled TRX lattices, uranium-oxide fueled BAPL lattices and Th^{232}-U^{233} fueled BNL lattices. The use of a new thermal scattering matrix for Hydrogen from ENDF/B-VI increased k_{eff} for 0.5 % while the use of ENDF/B-VI U^{238} decreased it for 2.5 %. Although the original WIMS library performed well for the effective multiplication factor of the lattices there is an improvement for the epithermal to thermal capture rate of U^{238} while using new data in the TRX and BAPL lattices.

The effect of the fission spectrum is investigated for the BNL lattices and it is shown that using U^{233} fission spectrum instead of the original U^{235} spectrum gives a k_{eff} which agrees better with the experimental value.

The results obtained by using new multigroup data are generally acceptable and in the experimental error range. They especially improve the prediction of the reaction rate dependent benchmark parameters.

Özet

ENDF/B-VI, JEF-2.2 ve JENDL-3 hesaplanmış nükleer veri kütüklerinin çok gruplu nükleer veri kütükleri formuna işlemek amacı ile NJOY nükleer veri işleme sistemi kullanıldı. Kullanılan veri kütüklerinin tarifi yapıldı ve verilerin işlenmesinde kullanılan varsayımlar sunuldu. Nükleer veri kütükleri arasındaki benzerlikler ve farklılıklar GROUPIE programı kullanılarak dört grup etkin tesir kesiti hesaplamak sureti ile incelendi. Ayrıca INTER programı kullanılarak resonans integralleri hesaplandı ve karşılaştırıldı. JEF ve ENDF/B-VI deki U^{238} verilerinin aynı olduğu gösterildi. Aynı şekilde JENDL ve ENDF/B-VI deki U^{235} verilerinin de benzer olduğu gösterildi.

NJOY tarafından oluşturulan çok gruplu nükleer veri kütüğünün WIMS-D4 programı ile uyumlu hale getirilmesi amacı ile çesitli programlar yazıldı ve işletildi. Oluşturulan çok gruplu veri kütüklerinin performans ve uygunluğunu test etmek için metal yakıtlı TRX örgüleri, uranium-oksit yakıtlı BAPL örgüleri ve Th^{232}-U^{233} yakıtlı BNL örgüleri kullanıldı. ENDF/B-VI verisi kullanılarak üretilen yeni Hidrojen termal saçılım matrisinin k_{eff} I 0.5 % arttırdığı gösterildi. Buna karşın ENDF/B-VI U^{238} in k_{eff} I 2.5 % azalttığı hesaplandı. Her ne kadar orijinal WIMS veri tabanı örgülerin efektif çarpım katsayısını hesaplama oldukca iyi sonuç versede yeni verilerin TRX ve BAPL örgüleri için U^{238} epitermal den termal'e yutma katsayısını iyileştirdiği gösterildi.

Fisyon spektrumunun etkisi BNL örgüleri için incelendi ve U^{235} fisyon spektrumu yerine U^{233} spektrumunun kullanılmasının deneysel değer ile daha uyumlu bir k_{eff} hesapladığı gösterildi.

Oluşturulan çok gruplu nükleer veri tabanları ile hesaplanan deneysel referans değerlerin genelde kabul edilebilir olduğu ve deneysel hata oranı sınırı içinde kaldığı gösterildi. Özellikle tepkime oranına bağlı referans parametrelerinin deneysel verile ile uyumunun önemli ölçüde iyileştiği gösterildi.

Acknowledgements

I wish to express sincere appreciation to my thesis adviser Dr. Cemal Niyazi Sökmen for his advice and support during the preparation of this thesis. I would also like to thank Dr. Osman Kemal Kadiroğlu and Dr. Mehmet Tombakoğlu for their help and valuable suggestions as committee members. I appreciate the help of Mine Kadiroğlu who read the draft and made valuable comments.

Contents

List of Figures vi

List of Tables vii

1 Introduction 1

2 Processing of Evaluated Data 6
- 2.1 Structure of ENDF File . . . 6
- 2.2 Resonance Region . . . 8
- 2.3 Doppler Broadening . . . 10
- 2.4 Transfer Matrix . . . 11
- 2.5 Multigroup Data . . . 13

3 Tools and Methods 18
- 3.1 Computational Resources . . . 18
- 3.2 Computer Programs . . . 18
  - 3.2.1 Module NJOY . . . 19
  - 3.2.2 Module MODER . . . 19
  - 3.2.3 Module RECONR . . . 19
  - 3.2.4 Module BROADR . . . 21
  - 3.2.5 Module UNRESR . . . 21
  - 3.2.6 Module THERMR . . . 21
  - 3.2.7 Module GROUPR . . . 22
  - 3.2.8 Module WIMSR . . . 22
  - 3.2.9 The WIMS Code . . . 22
  - 3.2.10 PRE-WIMS Processing Programs . . . 23
- 3.3 Data Libraries . . . 24
  - 3.3.1 ENDF/B-VI . . . 24
  - 3.3.2 JEF-2.2 . . . 25
  - 3.3.3 JENDL-3 . . . 25
  - 3.3.4 Comparison of Data Libraries . . . 25
  - 3.3.5 Runtime and Size of ENDF tapes . . . 33

4 Benchmark Problems **36**
4.1 TRX-1 and TRX-2 36
4.2 BAPL-1, BAPL-2 and BAPL-3 38
4.3 BNL-1, BNL-2 and BNL-3 39
4.4 Processing Considerations 40
4.4.1 Materials and Methods 40
4.4.2 Resonance Integral and Cross Sections 44

5 Results and Conclusion **46**
5.1 Sensitivity of TRX and BAPL lattices to U^{238} and Hydrogen 46
5.2 TRX-1 and TRX-2 47
5.3 BAPL-1, BAPL-2 and BAPL-3 50
5.4 BNL-1, BNL-2 and BNL-3 52
5.5 Effect on Fission Spectrum in the BNL Lattices 52
5.6 Conclusion 54

References **60**

A Index of Evaluated Nuclear Data Files **62**
A.1 Index of the ENDF/B-VI Nuclear Data File 62
A.2 Index of the JEF-2.2 Nuclear Data File 63
A.3 Index of the JENDL-3 Nuclear Data File 64

B NJOY Input Files **65**
B.1 Input File for U^{238} 65
B.2 Input File for U^{235} 67
B.3 Input File for U^{233} 68
B.4 Input File for Th^{232} 70
B.5 Input File for Aluminum 71
B.6 Input File for Oxygen 72
B.7 Input File for Hydrogen Bound in Water 73

C WIMS Inputs for Benchmark Assemblies **75**
C.1 TRX Input 75
C.2 BAPL Input 76
C.3 BNL Input 77

D Listing of Utility Programs **78**
D.1 Program Libdiv 78
D.2 Program Libgen 82

List of Figures

1.1 Calculational Flow Path 4
3.1 NJOY Modules Used in the Study 20
5.1 Normalized U^{233} Fission Spectra 55

List of Tables

3.1 Coarse group energy mesh used in comparison 26
3.2 4 Group Cross Sections for U^{238} 28
3.3 Average cross section values for U^{238} 29
3.4 4 Group Cross Sections for U^{235} 30
3.5 Average cross section values for U^{235} 31
3.6 4 Group Cross Sections for U^{233} 32
3.7 Average cross section values for U^{233} 33
3.8 4 Group Cross Sections for Th^{232} 34
3.9 Average cross section values for Th^{232} 35
3.10 CPU time and Disk Space requirements for NJOY 35

4.1 Physical Properties of the TRX-1 and TRX-2 lattices. 37
4.2 Experimental data for TRX-1 and TRX-2 lattices. 37
4.3 Physical Properties of the BAPL-1, BAPL-2 and BAPL-3 lattices. 38
4.4 Experimental data for the BAPL lattices. 38
4.5 Physical Properties of the BNL-1,BNL-2 and BNL-3 lattices 40
4.6 Experimental data for the BNL lattices. 40
4.7 Material numbers of the nuclides processed from the data libraries . 42

5.1 Sensitivity of TRX and BAPL lattices to H and U^{238} 48
5.2 Summary of benchmark parameters for TRX-1 48
5.3 Summary of benchmark parameters for TRX-2 50
5.4 Summary of benchmark parameters for BAPL-1 51
5.5 Summary of benchmark parameters for BAPL-2 51
5.6 Summary of benchmark parameters for BAPL-3 52
5.7 Summary of benchmark parameters for BNL-1 53
5.8 Summary of benchmark parameters for BNL-2 53
5.9 Summary of benchmark parameters for BNL-3 53
5.10 Results for different Fission Spectra 56

Chapter 1

Introduction

The Evaluated Nuclear Data Files are the basic source of standardized nuclear data for calculation of nuclear systems (1).

The data in an Evaluated Nuclear Data File normally cover the full energy range of interest (e.g. 10^{-5}eV to 20MeV) and include all neutron nuclear reactions occuring in this energy range. Since the data is tabulated in small neutron energy steps it contains a large number of points to represent the physical behavior of a reaction accurately (2). Another important feature of the nuclear data files is that they share a common file format that makes exchange and comparison between different files possible.

The complex structure and the size of the Evaluated Nuclear Data Files prevent them to be directly used in nuclear applications. Only some Monte Carlo programs which can read the data in pointwise representation use the Evaluated Nuclear Data File without any reduction technique. For other programs the data must be group averaged to a suitable form for the application of interest. Producing a multigroup library from evaluated nuclear data is a time consuming and difficult process. First the energy dependence of the nuclear data must be reconstruc-

ted and the data must be "broadened" to the desired temperatures. If necessary thermal scattering matrices must be generated. An appropriate weight spectrum and group structure must be chosen for the multigroup library and all this must be repeated for all materials of interest.

Until recently the processing of the evaluated data to multigroup form required very large computers which could handle the required computational power and disk storage. This prevented researchers with limited computational resources to use the evaluated data files directly to produce multigroup nuclear data libraries for their specific problem. With the advancement of high speed desktop computer systems and the availability of inexpensive hard disk storage systems the processing of evaluated nuclear data files are becoming a possibility for the researcher. Previously a researcher could only use the multigroup cross section libraries supplied with the application. Although this multigroup libraries are suitable for a specific range of problems they may fail to provide acceptable results for some other ones and the researcher is not able to change the group structure of the multigroup library. Other disadvantages of these libraries are that they are relatively old (WIMS library is more than 20 years old !) and that they do not incorporate recent changes to improve the accuracy of the nuclear data.

The generation of multigroup nuclear data for a application requires through knowledge of the problem and of the codes involved in the task. It is important to understand the assumptions and approximations made and the limitations of the produced multigroup library. The Cross Section Evaluation Working Group (CSEWG) maintains a set of benchmark lattices which can aid in verifying the work done and can give the researcher an initial indication of how well the generated multigroup library would be expected to perform in the application. These benchmark lattices are well documented and investigated by various laboratories around the world.

In view of the reasons cited above the main objectives of the work described in this thesis are:

- Installing Evaluated Nuclear Data Files and the necessary computer codes to process these data files on a specific Computer System.
- Using the NJOY code to provide a calculational path to process the evaluated data files into multigroup form. Applying various processing options and investigating the effects of these options.
- Providing several utility programs that maintain and convert the multigroup library produced by the NJOY code into WIMS-D4 form.
- Using the WIMS-D4 code to compare the suitability of the new multigroup libraries by modeling several benchmark lattices from the Cross Section Evaluation Working Group (CSEWG). Comparing several benchmark parameters with published results.

The calculational flow path used in the work is presented in Figure 1. The Evaluated Nuclear Data File for the material of interest is processed with NJOY using appropriate input data. The resulting mutigroup data file is converted into WIMS usable form with the use of auxiliary programs. After that WIMS is executed with appropriate input data for the specific problem.

The following evaluated data files were used in the study :

ENDF/B-VI: United States Evaluated Nuclear Data File. Coordinated and distributed by the Brookhaven National Laboratory.

JEF-2.2: Joint Evaluated File produced by NEA countries and coordinated by the NEA Data Bank.

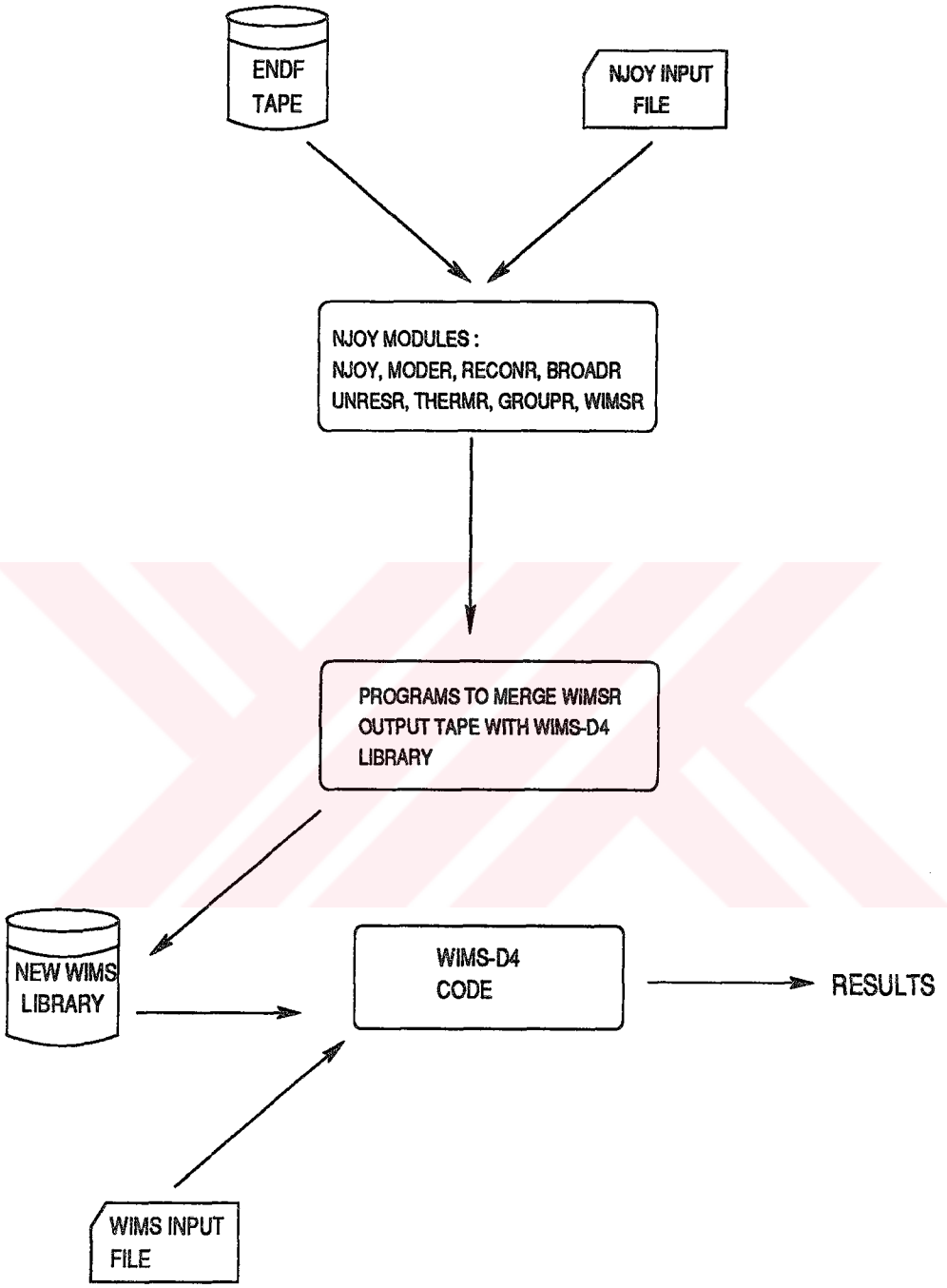

Figure 1.1: Calculational Flow Path

JENDL-3.2: Japanese Evaluated Nuclear Data Library. This data file is made available through the nuclear data section of the International Atomic Energy Agency.

The following chapter gives a brief introduction to the processing of evaluated nuclear data. The tools and methods used in the study is given in chapter 3 in which a brief introduction to the computational resources used is given and the data libraries are compared. Chapter 4 introduces the benchmark lattices and gives overview of processing considerations for the materials. A sensitivity analysis considering the individual effect of the new H^1 and U^{238} on the benchmark parameters of the TRX and BAPL lattices is given in the first part of chapter 5. The full set of results for the generated multigroup libraries is given in tabular form and are discussed. The effect of the fission spectrum is investigated for the BNL lattices. The conclusion and suggestions for future work is given in the last section of Chapter 5.

Chapter 2

Processing of Evaluated Data

The Evaluated Nuclear Data Files (ENDF) contain the necessary basic cross section data to perform reactor physics calculations. Any microscopic neutron cross section of interest is either directly represented in tabular form and resonance parameters or can be explicitly calculated using existing data (1).

2.1 Structure of ENDF File

As a function of neutron energy the ENDF data structure for a particular material is :

1. Tabulated representation at low energies up to the resonance region.
2. parametric representation plus a tabulated background cross section in resolved and unresolved resonance region.
3. Tabulated representation at high energies.

Interpolation between subsequent energy points is used to define the cross sections over the full energy range of interest. There are five different interpolation laws that are commonly used to represent the data in tabular form:

1. Constant values between two points (constant law).
2. Linear interpolation between cross section and energy points (linear-linear law).
3. Linear interpolation between cross section points, logarithmic interpolation in energy (linear-log law).
4. Logarithmic interpolation between cross section points, linear variation in energy (log-linear law).
5. Logarithmic interpolation between cross section and energy points (log-log law).

The use of interpolation laws is quite convenient and gives fairly accurate representation of the microscopic cross sections if applied properly. A common example to illustrate the effect of different interpolation laws is the 1/V cross section shape which can be exactly represented by the log-log interpolation law while representing the same region with linear-linear representation is vastly different and gives incorrect results.

The drawback of interpolation laws is that it is often not possible to accurately represent the sum of two or more reactions by the interpolation laws if any of the reactions uses log interpolation between data points. This is a problem if the ENDF file tabulates sums of reactions like the total cross section (e.g. so called "redundant" cross sections) which is the case in most of the evaluations. In this case the difference between the total cross section and the sums could be nonzero which would cause major problems in reactor physics calculations if this fact is not treated properly by the code used. A solution to this problem is to convert all interpolation laws into linearly interpolable form. The conversion of the constant law to linear form is accomplished by replacing a initial energy cross-section pair at a interval by two energy cross-section pairs; one at the lower limit and the other at the upper limit

of the interval. The linear law is already in the desired form. The interpolation laws including logarithmic forms are converted to linearly interpolable form by a technique called "interval halving". In this method each interval is divided in half until the value at the middle of the interval can be approximated by linear interpolation within a predefined error limit. The linearization of cross section data is also very useful for subsequent processing steps because dealing with only linear interpolation simplifies these steps considerably.

2.2 Resonance Region

The resonance region in a ENDF file is divided into a resolved and an unresolved part. This division arises because while the resonance parameters in the resolved region uniquely represent the energy-dependent cross section of interest, the parameters in the unresolved region represent only the distribution of cross sections and can as such only be used to calculate average values.

In the resolved region there are commonly four different kinds of parameters that can be used to represent resonance cross sections.

1. Single-level Breit-Wigner parameters (SLBW).
2. Multi-level Breit-Wigner parameters (MLBW).
3. Reich-Moore parameters.
4. Adler-Adler parameters.

The method generally used in reconstructing the energy-dependent cross section in the resolved resonance region is at first to use the total width of two adjacent resonances to divide the energy between the resonance into subintervals.

The length of these subintervals is determined by the total width of the nearest resonance. The interval between two wide closely spaced resonances is divided into a few subintervals while the interval of two narrow, widely spaced resonances is divided into many subintervals. These subintervals are then subdivided further using the iterative interval halving technique, until the cross section is linearly interpolable over each resulting interval up to a predefined error limit.

In ENDF evaluations, the unresolved range begins at an energy where it begins to get difficult to measure individual resonances and extends to an energy where the effects of fluctuations in the resonance cross sections become unimportant for practical calculations. Resonance information for this unresolved range is given as average values for resonance widths and spacings together with distribution functions for the widths and spacings. Effective cross sections are then calculated by calculating cross sections at the energy points at which unresolved parameters are given and then interpolating this cross sections to calculate the cross section at the energy point of interest.

The commonly used parameters in the unresolved region are:

1. Constant or energy-independent parameters.

2. Energy-dependent fission width, other widths constant.

3. All widths energy dependent.

After calculating and linearizing the resonance contribution the linearized background cross section must be added to it in order to get the actual energy-dependent cross section.

The methods discussed above are used in the RECONR and UNRESR modules of the NJOY code system in order to calculate resonance contributions and linearize all cross sections of interest for a material.

2.3 Doppler Broadening

The cross sections in the ENDF files are presented as function of neutron energy, where the neutron energy is measured relative to stationary (e.g. "cold") target nuclei. The cross sections are also called 0 Kelvin cross sections. However in all real cases the nuclei in a medium have a distribution of kinetic energies and are moving in a random fashion in a medium. In this case there will be for a distribution of randomly moving target nuclei a full spectrum of energies to be considered.

The "Doppler Broadening" approach is used to calculate from the "cold" cross section the actual cross section for a medium with nonstationary nuclei. In this approach the effective cross section for a material at a nonzero temperature is defined such that it gives the same reaction rate for stationary target nuclei as the real cross section gives for moving nuclei. The generalized Doppler Broadening equation is :

$$\overline{\sigma}(v) = \frac{\alpha^{1/2}}{\pi^{1/2} v^2} \int_0^\infty dV\, \sigma(V) V^2 \left\{ e^{-\alpha(V-v)^2} - e^{-\alpha(V+v)^2} \right\} . \tag{2.1}$$

where $\alpha = M/(2kT)$, k is Boltzmann's constant, and M is the target mass. V is the relative speed $V = v - v'$, v is the velocity of the incident particles, v' is the velocity of the target nuclei and σ is the cross section for stationary nuclei. Equation 2.1 can be broken up into two parts as :

$$\overline{\sigma}(v) = \sigma^*(v) - \sigma^*(-v) , \tag{2.2}$$

where

$$\sigma^*(v) = \frac{\alpha^{1/2}}{\pi^{1/2} v^2} \int_0^\infty dV\, \sigma(V) V^2 e^{-\alpha(V-v)^2} . \tag{2.3}$$

There are two well known properties of Doppler Broadening which originate from the fact that the broadening equation is actually a form of the diffusion equation. The first is that, if the temperature is increased the reaction rate will become smoother

and will asymptotically approach a constant or uniform distribution. This can be illustrated by the fact that a 1/V cross section, which corresponds to a already constant reaction rate is independent of temperature and remains unchanged during the broadening process. The second property of the broadening equation is that the integral of the reaction rate over all energy space is independent of the temperature .e.g. the total reaction rate is conserved.

One of the methods to evaluate the Doppler Broadening equation 2.1 and which is also used in the BROADR module of the NJOY system is the "Kernel Broadening" method. This method uses a numerical integration of equation 2.3 and is fully accurate with respect to all resonance and non-resonance cross sections. Another approach, which is called the psi-chi method, starts from resonance parameters and uses certain approximations to obtain an expression for the broadened cross section in terms of tabulated and calculated functions.

2.4 Transfer Matrix

The representation of the scattering cross section is different from the other cross section types because evaluated scattering data is represented in terms of the scattering angle and therefore one has to consider instead of cross section-energy pairs a scattering transfer matrix of the form :

$$\sigma(\mu_s, E' \rightarrow E) = m(E')\sigma(E')p(E', \mu_s, E' \rightarrow E)g(\mu_s, E' \rightarrow E) \tag{2.4}$$

where $m(E')$ is the muptiplicity of the reaction (.e.g. 1 for elastic and inelastic, 2 for (n,2n) and $\bar{\nu}(E)$ for fission), $\sigma(E')$ is the cross section for the reaction, $p(E', \mu_s)$ is the angular distribution as a function of incident energy and $g(\mu_s, E' \rightarrow E)$ is the energy distribution of the reaction.

In the evaluated library multiplicity $m(E')$ is either given explicitly, as for $\bar{\nu}(E)$,

or is implied by the reaction type. The angular distribution, $p(E', \mu_s)$, is either given in terms of Legendre coefficients or in tabulated form. The energy distribution, $g(\mu_s, E' \rightarrow E)$, is in the evaluations given in several ways which includes tabulation as a function of the secondary energy E, representation as a simple fission spectrum which depends on the incident energy, representation as a evaporation spectrum and representation as a energy dependent Watt Spectrum. It is shown in (1) that for all practical purposes these representations can be expressed as a linearly interpolable function of E'.

Neutron scattering at low thermal energies must be treated differently if the binding of the scatterer in a material or the motion of atoms in a gas is important. There are several cases which must be considered separately in such conditions; Coherent elastic scattering by crystalline materials, Incoherent elastic scattering by non-crystalline materials and Inelastic scattering for a gas of free atoms or for bound scatterers.

Coherent elastic scattering occurs in crystalline solids where the so-called "zero-phonon term" leads to interference scattering from the various planes of atoms of the crystals making up the solid, such like graphite or Be. There is no energy loss in such scattering. The coherent scattering cross section is either given as a function of energy and temperature, which is used in newer ENDF formats, or in terms of lattice constants, form factor formulas and Debye-Waller coefficients, which is common for older ENDF formats.

Incoherent elastic scattering is found in hydrogenous solids like polyethylene, which have an elastic (no energy loss) component of scattering arising from the "zero-phonon" term that can be treated in the incoherent approximation because of the large incoherent cross section of hydrogen. There is no energy loss in this case and the required parameters to calculate the effective incoherent elastic

cross section are characteristic bound cross sections and Debye-Waller coefficients which are tabulated in the evaluations.

For incoherent inelastic scattering the cross sections and energy-to-energy transfer matrices can be calculated from ENDF $S(\alpha,\beta)$ scattering functions which describe the binding of the scattering atom in a material and where α is the dimensionless momentum transfer and β is the dimensionless energy transfer. The scattering functions are either given in tabular forms as tables of S versus α for various values of β or by means of the so called "Short Collision Time" (SCT) approximation which defines the cross section in terms of a effective temperature which is either tabulated in the ENDF file or is included in the processing codes. It must be noted that ENDF $S(\alpha,\beta)$ functions are available only for a number of important moderator materials

The THERMR module of the NJOY code system uses the representations above for the thermal range in order to calculate effective scattering cross sections for materials of interest.

2.5 Multigroup Data

The final step in processing evaluated data is collapsing the linearized pointwise cross section into Multigroup form which is used by computer codes that calculate the distributions of neutrons in space and energy.

The general definition of the multigroup cross section, which is weighted by a moment of the flux is :

$$\overline{\sigma_{Rng}} = \frac{\int_{E_g}^{E_{g+1}} \sigma_R(E)\phi_n(E)dE}{\int_{E_g}^{E_{g+1}} \phi_n(E)dE} \tag{2.5}$$

where $\sigma_R(E)$ is the total cross section for any reaction R, (e.g., R = total,elastic, capture etc.) and $\phi_n(E)$ is the nth Legendre moment of the flux (e.g. 0= scalar flux,

1=scalar current). The energy dependent pointwise cross section for equation 2.5 is obtained by the methods discussed previously. In almost all cases the weighting flux ϕ_n is not known since it is the actual particle distribution to be calculated by the computer codes. But what is really needed to calculate group averaged cross sections is not ϕ itself but rather the shape of ϕ and it is possible to calculate fairly accurate group averaged cross sections if the shape is reasonably well known over broad energy ranges of a few group structure or if a large number of groups are used so that the error in guessing the shape inside a group is not important. Another problem in evaluating equation 2.5 is that in many cases of interest, the flux ϕ will contain dips corresponding to the absorption resonances of the various materials in the problem. For the reaction rate $\sigma(E)\times\phi(E)$, these dips clearly reduce (e.g. self shield) the effect of the corresponding resonance and cause that the actual cross section for the resonance varies considerably from the unshielded value. It is possible to define the flux in equation 2.5 as :

$$\phi_n(E) = M_n(E) \times W_n(\sigma) \tag{2.6}$$

where $M_n(E)$ is the energy-dependent weighting spectrum and $W_n(\sigma)$ is a cross section dependent self-shielding factor. The energy dependent weighting spectrum is generally given in the processing codes either as a option from a number of built-in spectrums or is read-in from a user prepared input file. The important point in evaluating the self-shielding factor is that it is changing inversely with cross sections. This is an important result of the narrow, intermediate and wide resonance approximations . In view of that the weighting function ϕ can be actually assumed of the form:

$$\phi(E) = \frac{M(E)}{[\sigma_t(E) + \sigma_0]^k} : k = 0,1,2,... \tag{2.7}$$

where $M(E)$ is the energy dependent spectrum, $\sigma_t(E)$ is the total cross section of the material of interest, σ_0 is total cross section of all other constituents of the mix-

ture and k is an integer for different Legendre moments (e.g. k=0 means no self-shielding, 1 means self-shielded scalar flux, 2 means self-shielded scalar current etc.). The value of σ_0 actually gives the atom ratio of absorber and moderator materials and as such can have values from 0 (no moderator material) up to infinity (infinite diluted absorber material). This approach to self-shielding is called the "Bondarenko" model and is generally used in virtually any code that processes evaluated data into multigroup form. In case of strong heterogeneity effects the Bondarenko method can be extented by starting by an infinite system of moderator and fuel regions. In this case the neutron balance equations are

$$V_f \Sigma_f \phi_f = (1 - P_f) V_f S_f + P_m V_m S_m \,, \tag{2.8}$$

and

$$V_m \Sigma_m \phi_m = P_f V_f S_f + (1 - P_m) V_m S_m \,, \tag{2.9}$$

where V_f and V_m are the region volumes, Σ_f and Σ_m are the corresponding total macroscopic cross sections, S_f and S_m are the sources per unit volume in each region, P_f is the probability that a neutron born in the fuel will suffer its next collision in the moderator, and P_m is the probability that a neutron born in the moderator will suffer its next collision in the fuel. Using the reciprocity theorem,

$$V_f \Sigma_f P_f = V_m \Sigma_m P_m \,, \tag{2.10}$$

and the Wigner rational approximation to the fuel escape probability,

$$P_f = \frac{\Sigma_e}{\Sigma_e + \Sigma_f} \,, \tag{2.11}$$

where Σ_e is a slowly-varying function of energy called the escape cross section, one can obtain an equation for the fuel flux of the form

$$(\Sigma_f + \Sigma_e)\phi_f = \frac{\Sigma_e S_m}{\Sigma_m} + S_f \,. \tag{2.12}$$

It can be shown that in the limit where the resonances are narrow with respect to both fuel and moderator scattering, the source terms S_f and S_m take on their asymptotic forms of Σ_p/E and Σ_m/E respectively, and that this equation becomes equivalent to the Bondarenko model quoted above with

$$\sigma_0^f = \frac{\Sigma_e}{\rho_f}, \tag{2.13}$$

and

$$C(E) = \frac{\Sigma_e + \Sigma_p}{\rho_f E}. \tag{2.14}$$

The common method of evaluating equation 2.12 is to create libraries for a variety of σ_0 values (normally in powers of 10 e.g. 0, 10, 100, 1000 etc.) and then interpolate the cross sections for the desired value of σ_0. The Bondarenko method is used in the GROUPR module of the NJOY system to calculate self-shielded multigroup cross sections for a material. Optionally GROUPR can also use the so called "flux-calculator" approach in which a weighting flux is computed for various mixtures of heavy absorbers with light moderators, for calculating self-shielding effects. The flux-calculator option is especially useful for thermal reactor problems which normally have many broad and intermediate-width resonances in the thermal range which cannot be self-shielded with enough accuracy using the Bondarenko method. By considering an infinite homogeneous mixture of two materials and assuming that scattering is isotropic in the center-of-mass system we can write the integrals slowing down equation as

$$\sigma_t(E)\phi(E) = \int_E^{E/\alpha_1} \frac{\sigma_{s1}(E')}{(1-\alpha_1)E'}\phi(E')\,dE' + \int_E^{E/\alpha_2} \frac{\sigma_{s2}(E')}{(1-\alpha_2)E'}\phi(E')\,dE'. \tag{2.15}$$

where α is $(\frac{A-1}{A+1})^2$, A is the nuclear mass number. Assuming that material 1 is a pure scatterer with constant cross section and converting to the σ_0 (.e.g. simply assuming that $\sigma_t = \sigma_0 + \sigma_{t2}$) form the equation 2.15 can be written as

$$[\sigma_0+\sigma_{t2}(E)]\phi(E) = \int_E^{E/\alpha_1}\frac{\sigma_0}{(1-\alpha_1)E'}\phi(E')\,dE' + \int_E^{E/\alpha_2}\frac{\sigma_{s2}(E')}{(1-\alpha_2)E'}\phi(E')\,dE', \quad (2.16)$$

Assuming that material 1 (e.g the moderator) is so light that all the resonances of material 2 are narrow with respect to scattering from material 1 allows the first integral to be approximated by its asymptotic form 1/E, e.g. the integral is assumed to be a smooth function of E given by C(E). In this way, material 1 can represent a mixture of other materials just as in the Bondarenko method. Fission source and thermal upscatter effects can also be lumped in C(E). Following this the integral equation is now reduced to

$$[\sigma_0+\sigma_t(E)]\phi(E) = C(E)\sigma_0 + \int_E^{E/\alpha}\frac{\sigma_s(E')}{(1-\alpha)E'}\phi(E')\,dE', \quad (2.17)$$

It can be seen that in order to calculate the weighting flux ϕ in equation 2.17 the only unknown is σ_0 which must be provided by the processing code as an input option.

An important point in collapsing into multigroup form is the group ordering of the resulting multigroup library. The multigroup data libraries used with transport codes usually number the groups in such a way that group 1 is the highest energy group and all the scattering matrix elements that transfer neutrons into group 1 are given first, followed by those for scattering into group 2, and so on. But the evaluated nuclear data in ENDF files is given in order of increasing neutron energy and secondary neutron distributions are described by giving emission spectra for given neutron energies. Therefore, GROUPR numbers its groups such that group 1 is the lowest-energy group, and it calculates that scattering out of group 1, followed by the scattering out of group 2, and so on. The output modules of the NJOY system (WIMSR, ACER etc.) then rearrange the output into the conventional decreasing order group structure.

Chapter 3

Tools and Methods

3.1 Computational Resources

The Computational facilities in the Department of Nuclear Engineering presently available are exploited in the study. A Unix workstation from Silicon Graphics Computer Systems with a R4000 RISC chip, 32MByte of main memory and 2.5 GByte online disk storage is used to install the libraries and programs and make the necessary computer runs to produce the results.

3.2 Computer Programs

The NJOY code version 91.103 and the WIMS-D4 code were the primary programs used in the study. The NJOY Nuclear Data Processing System (8) is used as a general purpose link between ENDF-formatted evaluated nuclear data files and reactor physics applications. It has been under continuous development at the Los Alamos National Laboratory since 1974 (11). It is a highly modular system with a large spectrum of possible applications. The programming philosophy of the code makes it possible to include changes in a straightforward manner. The main-

tenance of the code is made through a update program which allows a change to the code to be performed trough a update file. Each module of the NJOY system communicates through the reading and writing of sequential files which makes in fact each module a separate program. Of the many modules of the NJOY system those which are used in the study are shown in Figure 3.1 and explained in the following sections.

3.2.1 Module NJOY

This NJOY module is the main driver of the program. It starts by reading an input option parameter which controls the nature of the run e.g. interactive or batch. and the ENDF version value. Then it reads the module name and loads the appropriate module.

3.2.2 Module MODER

The main purpose of the MODER module is the conversion of the data files to and from ASCII and binary format. It is also used to merge several tapes to a single one. It is often the first module called in the NJOY system after the main program because computers can deal with binary files much faster then with files in ASCII format.

3.2.3 Module RECONR

The cross section dependence in the resonance region is normally given in the form of parameters which are tabulated in a special section of the evaluated file. This is done to reduce space and to give a better representation of the resonance behavior. The RECONR module is used to reconstruct explicitly the energy dependence of the cross section from the resonance parameters and write

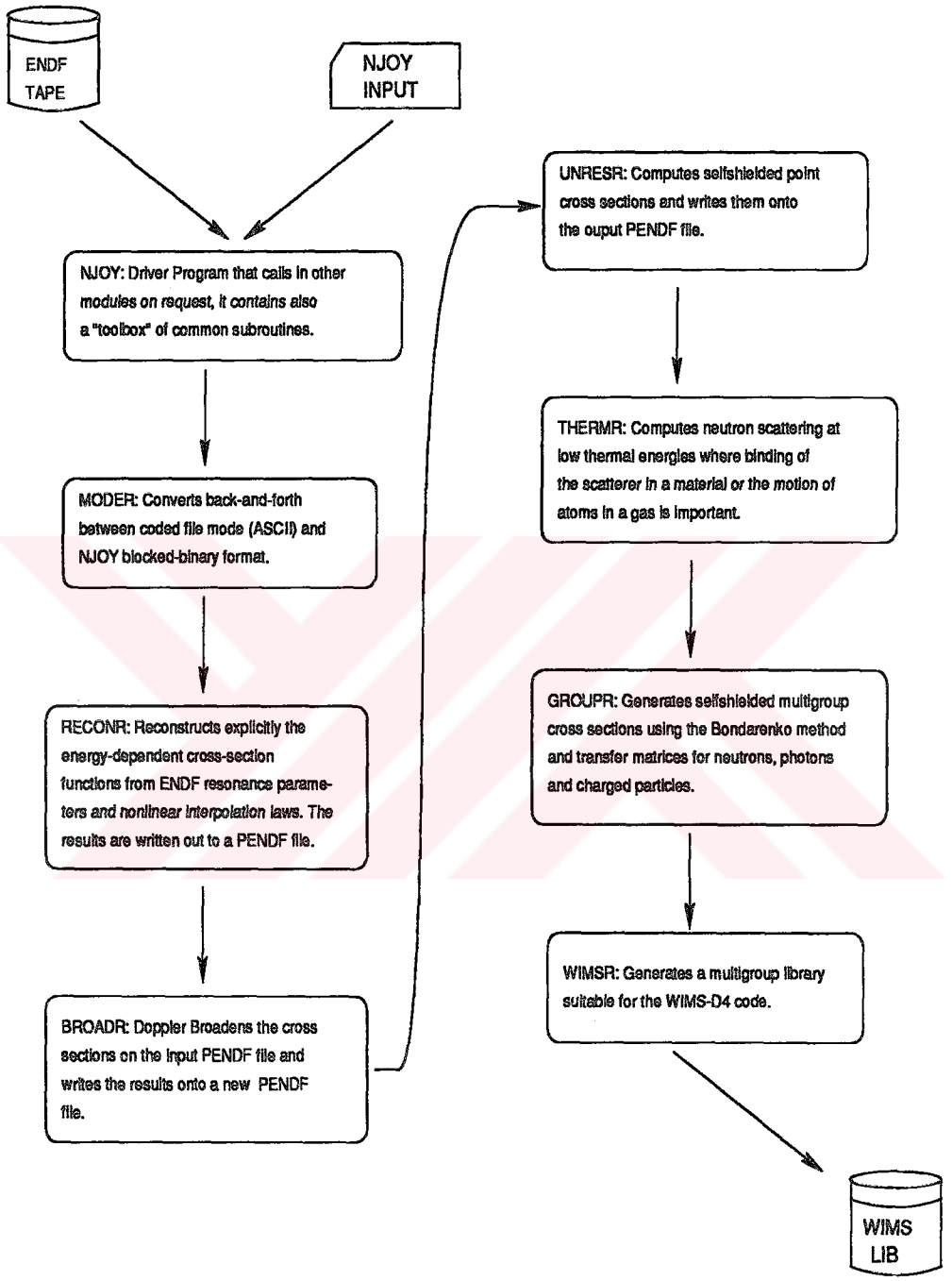

Figure 3.1: NJOY Modules Used in the Study

the results to a pointwise evaluated nuclear data file (PENDF). The size of the generated PENDF file and the run time required by the module is directly related to the fractional error value given by the user.

3.2.4 Module BROADR

The values on the ENDF file are calculated with reference to a single temperature (e.g. $0°K$). The BROADR module Doppler broadens the cross sections on the input PENDF file to the temperatures of interest and writes them into a new PENDF file. The accurate kernel broadening method is used in the process. The run time of the BROADR module is again dependent on the fractional error value given by the user.

3.2.5 Module UNRESR

This module computes self-shielded point cross sections and writes them to a PENDF file. It uses an analytic method to accomplish this. The cross sections are tabulated versus temperature T and background cross section (σ_0).

3.2.6 Module THERMR

The generation of the pointwise neutron scattering cross sections in the thermal range requires the use of the THERMR module. The module uses several methods to give an accurate representation of the scattering cross section for the material of interest. The results are written on a new PENDF file for use in subsequent modules.

3.2.7 Module GROUPR

The most important module in the process of generating multigroup cross section libraries is GROUPR (8) It uses the Bondarenko or Nordheim Integral method (1) to generate self-shielded multigroup neutron cross sections. It has various built-in weighting flux choices and multigroup library options. The user may supply an external weighting flux or library structure. The results are written out to a Group Evaluated Nuclear Data File (GENDF).

3.2.8 Module WIMSR

The WIMSR module is used to convert the groupwise ENDF produced by the GROUPR module in a form that can be used in the reactor physics code WIMS (12). The version used in the study is incorporating the changes by Trkov (10).

3.2.9 The WIMS Code

The Winfrith Improved Multigroup Scheme (WIMS) code originated from the UK laboratory AEE/Winfrith and is one of the most widely used programs for reactor physics and especially thermal reactor calculations. It contains a collision-probability lattice-cell transport and S_N code and the associated library. WIMS requires transport, fission, and capture cross-sections, a transfer matrix for epithermal neutrons, fission source information ($\bar{\nu}$ and χ), P1 matrices for several moderators, slowing down power, resonance tables, Goldstein-Cohen parameters (λ) and a bound-atom scattering matrix for thermal neutrons in order to compute fluxes in reactor pin cells.

The WIMS libraries normally use a standard 69-group structure with 14 fast groups, 13 resonance groups, and 42 thermal groups. The version used in this study is known as WIMS-D4 and is freely available through various distribution centers, mainly

NEA Data Bank. The libraries supplied with the code are originating from the early sixties and are mostly obsolete. Despite this the WIMS code performs surprisingly well while calculating benchmark problems. The main reason is that several adjustments were made, especially to the resonance integrals in the multigroup library. The adjustments were performed by comparison of the calculated integral parameters with measurements for a wide range of benchmark lattices. It is obvious that, although good results are obtained for a range of problems, the performance of the code can be improved with up to date data from current evaluations. The WIMS input to model the benchmark lattices is taken from Reference (10)

3.2.10 PRE-WIMS Processing Programs

Two small computer programs, which are presented in the appendix, were written in order to incorporate the produced multigroup library for a specific element into the WIMS library and maintain the library.

- The Libdiv program splits the original WIMS library into many files each containing a single material. Each file is complete and consistent. There is no data loss during the splitting process.

- The Libgen program produces a Binary WIMS library from the individual files. The user can select the number of elements to be included in the produced library. The non-standard structure of WIMSR generated multigroup files is taken into account and processed appropriately.

In order to produce a new WIMS multigroup library the NJOY code with appropriate input data and the necessary Evaluated Nuclear Data File is executed. Than the generated multigroup file in WIMS format is pasted into the existing WIMS

library via the PRE-WIMS processing programs. Finally WIMS is executed to investigate the benchmark problems.

3.3 Data Libraries

The following nuclear data libraries were retrieved from the NEA Data Bank in Saclay/France.

The data in the evaluated nuclear data files are indexed by material (MAT), type of information (MF), and reaction (MT). Materials can be single isotopes, elements, or compounds. Type of information includes resonance parameters (MF=2), energy-dependent cross section (MF=3), angular distributions (MF=4), secondary energy distributions (MF=5), and energy-angle distributions (MF=6).

Although a detailed description of the data files can be found elsewhere (3) (4) a brief description is given below.

3.3.1 ENDF/B-VI

The Evaluated Nuclear Data File version VI is the latest version of a number of evaluations originating in the mid sixties. It is distributed through the National Nuclear Data Center (NNDC) at the Brookhaven National Laboratory, USA. It includes mainly evaluations made by the US National Laboratories and as such is considered as fairly precise and complete. The ENDF/B library version IV which was released in 1974 is still one of the most widely used evaluations (7). The ENDF/B-VI files contain a number of new features of interest to reactor physics applications. For example the resonance ranges of U^{235},U^{238} and Pu^{239} are extended to higher energies to minimize problems with the unresolved range (9). The ENDF/B-VI library also includes error estimates in the form of covariance matrices which can be used to study the

sensitivity of predicted reactor parameters to evaluated data uncertainties. The full content of the ENDF/B-VI file used in the study is given in Appendix A.1.

3.3.2 JEF-2.2

The Joint Evaluated File version 2.2 is produced by the NEA countries through a project coordinated by the NEA Data Bank (7). It is a general purpose library which contains data compiled and evaluated in several European countries, mainly France, Germany and United Kingdom. It is well documented and has radioactive decay data for more than 2300 isotopes. A detailed verification study is conducted through various European laboratories and new improvements are included gradually in the library. The content of the JEF-2.2 file used in the study is given in Appendix A.2. This file is only a subset containing the necessary heavy elements.

3.3.3 JENDL-3

The Japanese Evaluated Nuclear Library version 3 is a general purpose library produced and distributed by the Japanese Atomic Energy Institute (JAERI). It contains evaluations coming from Japanese laboratories and covers 7 different areas; Dosimetry file, Gas-production cross section data file, Activation cross section file, Decay data file, Fusion file, (α, n) reaction file, and KERMA file. The content of the JENDL-3 file used in this study is given in appendix A.3. This file is a subset of the full JENDL-3 evaluation.

3.3.4 Comparison of Data Libraries

In order to compare the data libraries 4 group cross sections for U^{238}, U^{235}, U^{233} and Th^{232} was generated with the aid of the ENDF Preprocessing Codes of D. E. Cullen (5). The codes LINEAR, RECENT, SIGMA1, FIXUP and GROUPIE were used

Table 3.1: Coarse group energy mesh used in comparison

Group	Upper	Lower
4	2 MeV	67.379 KeV
3	67.379 KeV	3.355 KeV
2	3.366 KeV	0.625 eV
1	0.625 eV	0 eV

for this purpose. The code LINEAR linearizes the ENDF data (.i.e. converts all nonlinear tabulations to linear form). RECENT reconstructs the resonance dependence from the parameters in file 2 (MF=2) of the ENDF data. SIGMA1 calculates cross sections for a given temperature (in our case 300^0K). FIXUP checks the generated data for inconsistency and GROUPIE generates few group cross sections for the given ENDF data. The group energy mesh used to collapse the cross sections is shown in Table 3.1. The spectrum used to condense the cross sections was Maxwellian for the thermal range, 1/E for the intermediate range (up to 67 KeV) and fission spectrum for above 67 KeV.

The program INTER (6) from the ENDF Utility Codes of C. L. Dunford was used to verify the results of GROUPIE. INTER calculates, cross sections at 2200 m/s (σ_{2200}), Maxwellian averaged thermal cross sections ($\bar{\sigma}$), resonance integrals (I_R) and fission spectrum averaged cross sections (σ_{fiss}) from a given ENDF data file. The Maxwellian averaged cross sections are listed at 0.0253 eV and the resonance integral calculation is performed between 0.5 eV and 100.0 KeV. The fission spectrum calculation is done for a temperature of 1.02E+6 eV and the integration is made from 1.0KeV to 20.0 MeV.

Comparison for U^{238}

The generated 4 group cross sections for U^{238} is given in Table 3.2, which lists the total, elastic, capture and fission cross sections in terms of un-shielded average values and shielded Bondarenko f factors. The f factors are tabulated for approximately 50 barn (e.g σ_{50b}) , total shielded ($\frac{1}{\Phi}$) and current shielded ($\frac{1}{P_{si}}$).

The table shows that the ENDF/B-VI and JEF-2.2 evaluations have principally the same data. Only GROUP 4 shows a very small difference between the two evaluations with a average total cross section of 6.7515 barn for ENDF/B-VI versus 6.7697 barn for JEF-2.2. The data for JENDL-3 also shows very similar results with ENDF/B-VI and JEF-2.2 for the first 2 groups.

The INTER results given in Table 3.3 verify our conclusion. The ENDF/B-VI and JEF-2.2 values show that the data is the same for U^{238}. There is only a small difference for the cross sections in the fission region. The JENDL-3 cross sections are a little bit larger than that of JEF-2,2 and ENDF/B-VI with a total cross section of 12.1828 barn for JENDL-3 versus 12.172 barn for both ENDF/B-VI and JEF-2.2.

Comparison for U^{235}

The calculated 4 group cross sections for U^{235} in Table 3.4 show that for these material the tabulated data differs considerably between ENDF/B-VI and JEF-2.2. The group 1 total cross section is 6575.9 barn for JEF-2.2 while it is 6730 barn for both ENDF/B-VI and JEF-2.2. The calculated cross sections from ENDF/B-VI and JENDL-3 are the same in group 1 and group 2.

The INTER results for U^{235} in table 3.5 verify that for the ENDF/B-VI data and JENDL-3 data are the same for thermal cross sections. The resonance integral for JENDL-3 has a smaller value than ENDF/B-VI and JEF-2.2 which may account for the difference seen in the 4 group cross sections. The fission region data for ENDF/B-VI

Table 3.2: 4 Group Cross Sections for U^{238}

ENDF/B-VI	REACT	AVERAGES	σ_{50b}	$\frac{1}{\Phi}$	$\frac{1}{\Phi_{ai}}$
1	σ_t	3.7366+ 1	0.83627	0.49767	0.36471
	σ_s	1.2657+ 1	0.92813	0.79888	0.75595
	σ_γ	2.4709+ 1	0.78922	0.34337	0.16430
2	σ_t	7.8257+ 1	0.24167	0.13313	0.10906
	σ_s	3.5346+ 1	0.36851	0.25819	0.21413
	σ_γ	4.2911+ 1	0.13720	0.03011	0.02251
3	σ_t	1.6037+ 1	0.82447	0.71217	0.51568
	σ_s	1.4638+ 1	0.83665	0.72544	0.52010
	σ_γ	1.0553+ 0	0.58351	0.37524	0.28682
4	σ_t	6.7517+ 0	0.99805	0.99055	0.98156
	σ_s	3.6848+ 0	0.99744	0.98740	0.97520
	σ_γ	2.5070- 2	0.98537	0.92528	0.85010
	σ_f	8.3950- 1	1.00857	1.04223	1.08295
JEF-2.2	REACT	AVERAGES	σ_{50b}	$\frac{1}{\Phi}$	$\frac{1}{\Phi_{ai}}$
1	σ_t	3.7366+ 1	0.83627	0.49767	0.36471
	σ_s	1.2657+ 1	0.92813	0.79888	0.75595
	σ_γ	2.4709+ 1	0.78922	0.34337	0.16430
2	σ_t	7.8257+ 1	0.24167	0.13313	0.10906
	σ_s	3.5346+ 1	0.36851	0.25819	0.21413
	σ_γ	4.2911+ 1	0.13720	0.03011	0.02251
3	σ_t	1.6041+ 1	0.82454	0.71216	0.51551
	σ_s	1.4680+ 1	0.83727	0.72669	0.52135
	σ_γ	1.0554+ 0	0.58361	0.37538	0.28690
4	σ_t	6.7697+ 0	0.99811	0.99081	0.98205
	σ_s	3.6998+ 0	0.99785	0.98937	0.97905
	σ_γ	2.4506- 2	0.98628	0.92928	0.85739
	σ_f	8.3941- 1	1.00836	1.04124	1.08111
JENDL-3	REACT	AVERAGES	σ_{50b}	$\frac{1}{\Phi}$	$\frac{1}{\Phi_{ai}}$
1	σ_t	3.7374+ 1	0.83634	0.49788	0.36492
	σ_s	1.2665+ 1	0.92819	0.79908	0.75618
	σ_γ	2.4709+ 1	0.78926	0.34349	0.16438
2	σ_t	7.8260+ 1	0.24170	0.13315	0.10909
	σ_s	3.5349+ 1	0.36855	0.25824	0.21418
	σ_γ	4.2911+ 1	0.13720	0.03011	0.02251
3	σ_t	1.5938+ 1	0.82322	0.71308	0.51918
	σ_s	1.4571+ 1	0.83590	0.72766	0.52524
	σ_γ	1.0536+ 1	0.58196	0.37515	0.28772
4	σ_t	6.7455+ 0	0.99800	0.99016	0.98065
	σ_s	3.5826+ 0	0.99671	0.98376	0.96800
	σ_γ	2.4449- 2	0.98383	0.91886	0.83882
	σ_f	8.2728- 1	1.00860	1.04223	1.08270

Table 3.3: Average cross section values for U^{238}

ENDF/B-VI	σ_{2200}	$\bar{\sigma}$	I_R	σ_{fiss}
σ_t	1.21727E+01	1.1870E+01	5.96974E+02	7.62806E+00
σ_s	9.44319E+00	9.4403E+00	3.19107E+02	4.57007E+00
σ_{in}	0.00000E+00	0.0000E+00	2.18103E-01	2.66730E+00
σ_f	0.00000E+00	0.0000E+00	2.15605E-03	3.16017E-01
σ_γ	2.72946E+00	2.4302E+00	2.77648E+02	6.55626E-02
JEF-2.2	σ_{2200}	$\bar{\sigma}$	I_R	σ_{fiss}
σ_t	1.21727E+01	1.1870E+01	5.96974E+02	7.64809E+00
σ_s	9.44319E+00	9.4403E+00	3.19107E+02	4.51483E+00
σ_{in}	0.00000E+00	0.0000E+00	2.18103E-01	2.74490E+00
σ_f	0.00000E+00	0.0000E+00	2.15607E-03	3.16052E-01
σ_γ	2.72946E+00	2.4302E+00	2.77648E+02	6.47738E-02
JENDL-3	σ_{2200}	$\bar{\sigma}$	I_R	σ_{fiss}
σ_t	1.21828E+01	1.1880E+01	5.96192E+02	7.64967E+00
σ_s	9.45336E+00	9.4500E+00	3.18360E+02	4.55264E+00
σ_{in}	0.00000E+00	0.0000E+00	1.94030E-01	2.70654E+00
σ_f	0.00000E+00	0.0000E+00	1.89235E-03	3.21232E-01
σ_γ	2.72944E+00	2.4301E+00	2.77633E+02	6.17301E-02

and JEF-2.2 is almost identical.

Comparison for U^{233}

For U^{233} the calculated 4 group cross sections given in Table 3.6 show that for group 1 and group 2 the cross sections from JENDL-3 are larger than ENDF/B-VI and JEF-2.2. The total cross section in group 1 is 5309.1 for JENDL-3 while it is 5215.3 barn for JEF-2.2 and 5242 barn for ENDF/B-VI. The capture cross section in group 4 is 0.01451 barn for ENDF/B-VI versus 0.0201 barn for JEF-2.2 and 0.02 barn for JENDL-3.

The INTER results given in Table 3.7 shows that the thermal total cross section in JENDL-3 is higher than both ENDF/B-VI and JEF-2.2 which verifies the results of GROUPIE for group 1. The fission region total cross section in ENDF/B-VI and JENDL-3 are close to each other while JEF-2.2 has smaller values.

Table 3.4: 4 Group Cross Sections for U^{235}

ENDF/B-VI.	REACT	AVERAGES	σ_{50b}	$\frac{1}{\phi}$	$\frac{1}{P_{sl}}$
1	σ_t	6.7130+ 3	0.74011	0.10518	0.03192
	σ_s	2.0362+ 1	0.91061	0.73047	0.70776
	σ_γ	1.0640+ 3	0.73869	0.10012	0.02670
	σ_f	5.6287+ 3	0.73976	0.10388	0.03046
2	σ_t	6.7924+ 1	0.81747	0.54066	0.39584
	σ_s	1.2898+ 1	0.98581	0.96030	0.94405
	σ_γ	1.9059+ 1	0.72052	0.37518	0.22231
	σ_f	3.5967+ 1	0.80847	0.47787	0.29120
3	σ_t	1.6829+ 1	0.95841	0.85284	0.75806
	σ_s	1.0800+ 1	0.98491	0.92472	0.85284
	σ_γ	1.5255+ 0	0.89614	0.65862	0.46703
	σ_f	4.2370+ 0	0.90528	0.69704	0.53555
4	σ_t	6.6806+ 0	0.99814	0.99105	0.98259
	σ_s	3.5403+ 0	0.99747	0.98776	0.97616
	σ_γ	2.7029- 2	0.98808	0.93824	0.87504
	σ_f	1.5674+ 0	1.00391	1.01906	1.03727
JEF-2.2	REACT	AVERAGES	σ_{50b}	$\frac{1}{\phi}$	$\frac{1}{P_{sl}}$
1	σ_t	6.5759+ 3	0.74088	0.10747	0.03293
	σ_s	2.0439+ 1	0.91112	0.73603	0.71612
	σ_γ	1.0731+ 3	0.73865	0.10113	0.02726
	σ_f	5.4823+ 3	0.74068	0.10636	0.03149
2	σ_t	6.7837+ 1	0.82001	0.54333	0.39786
	σ_s	1.2999+ 1	0.98618	0.96052	0.94408
	σ_γ	1.8891+ 1	0.72538	0.38128	0.22729
	σ_f	3.5947+ 1	0.80965	0.47762	0.28996
3	σ_t	1.6815+ 1	0.95851	0.85272	0.75781
	σ_s	1.0780+ 1	0.98498	0.92477	0.85298
	σ_γ	1.5411+ 0	0.89551	0.65646	0.46416
	σ_f	4.2272+ 0	0.90596	0.69794	0.53641
4	σ_t	6.6815+ 0	0.99815	0.99106	0.98262
	σ_s	3.5411+ 0	0.99747	0.98779	0.97621
	σ_γ	2.7036- 2	0.98810	0.93835	0.87524
	σ_f	1.5674+ 0	1.00391	1.01906	1.03727
JENDL-3	REACT	AVERAGES	σ_{50b}	$\frac{1}{\phi}$	$\frac{1}{P_{sl}}$
1	σ_t	6.7130+ 3	0.74011	0.10518	0.03192
	σ_s	2.0362+ 1	0.91061	0.75252	0.70776
	σ_γ	1.0640+ 3	0.73869	0.10012	0.02670
	σ_f	5.6287+ 3	0.73976	0.10388	0.03046
2	σ_t	6.7924+ 1	0.81745	0.54060	0.39574
	σ_s	1.2898+ 1	0.98582	0.96029	0.94401
	σ_γ	1.9134+ 1	0.72145	0.37646	0.22344
	σ_f	3.5892+ 1	0.80813	0.47728	0.29057
3	σ_t	1.6747+ 1	0.96875	0.86993	0.77185
	σ_s	1.0896+ 1	0.98735	0.92812	0.85428
	σ_γ	1.4229+ 0	0.92117	0.70203	0.50571
	σ_f	4.1717+ 0	0.92918	0.73427	0.56345
4	σ_t	6.7357+ 0	0.99809	0.99077	0.98199
	σ_s	3.5688+ 0	0.99687	0.98477	0.97023
	σ_γ	2.3324- 2	0.98771	0.93568	0.86916
	σ_f	1.6095+ 0	1.00403	1.01963	1.03833

Table 3.5: Average cross section values for U^{235}

ENDF/B-VI	σ_{2200}	$\bar{\sigma}$	I_R	σ_{fiss}
σ_t	7.00596E+02	6.1224E+02	5.57480E+02	7.49678E+00
σ_s	1.51153E+01	1.5044E+01	1.52353E+02	4.19342E+00
σ_{in}	0.00000E+00	0.0000E+00	1.37531E-01	2.00655E+00
σ_f	5.86247E+02	5.0992E+02	2.72172E+02	1.20624E+00
σ_γ	9.92338E+01	8.7279E+01	1.32818E+02	8.25468E-02
JEF-2.2	σ_{2200}	$\bar{\sigma}$	I_R	σ_{fiss}
σ_t	6.97568E+02	6.0779E+02	5.57057E+02	7.49658E+00
σ_s	1.51923E+01	1.5083E+01	1.52910E+02	4.19320E+00
σ_{in}	0.00000E+00	0.0000E+00	1.37529E-01	2.00655E+00
σ_f	5.83386E+02	5.0605E+02	2.71941E+02	1.20624E+00
σ_γ	9.89888E+01	8.6650E+01	1.32070E+02	8.25619E-02
JENDL-3	σ_{2200}	$\bar{\sigma}$	I_R	σ_{fiss}
σ_t	7.00596E+02	6.1224E+02	5.56829E+02	7.56091E+00
σ_s	1.51153E+01	1.5044E+01	1.53008E+02	4.38235E+00
σ_{in}	0.00000E+00	0.0000E+00	1.54891E-01	1.86656E+00
σ_f	5.86247E+02	5.0992E+02	2.71208E+02	1.22745E+00
σ_γ	9.92338E+01	8.7279E+01	1.32459E+02	7.67146E-02

Comparison for Th^{232}

The 4 group cross section generated for Th^{232} are given in Table 3.8. The capture cross section in group 1 is almost the same for both ENDF/B-VI and JENDL-3 while the value of JEF-2.2 is slightly smaller. The capture cross sections calculated for group 2 are very close for all three evaluations. The group 4 fission cross sections are also very close with 0.31 barn for JENDL-3, 0.289 barn for JEF-2.2 and 0.299 barn for ENDF/B-VI.

The results of INTER show that the total thermal cross section data of JEF-2.2 is smaller than that of ENDF/B-VI and JENDF-3. The total resonance integral in JEF-2.2 is also lower for JEF-2.2 being 272.68 versus 303.5 for ENDF/B-VI and 308.9 for JENDL-3. The fission region cross section of JEF-2.2 has again smaller values than the other two evaluations.

Table 3.6: 4 Group Cross Sections for U^{233}

ENDF/B-VI	REACT	AVERAGES	σ_{50b}	$\frac{1}{\Phi}$	$\frac{1}{P_{gi}}$
1	σ_t	5.2420+ 3	0.74336	0.13413	0.05204
	σ_s	1.7247+ 1	0.90724	0.70598	0.66956
	σ_γ	4.1120+ 2	0.74361	0.13596	0.05339
	σ_f	4.8136+ 3	0.74275	0.13193	0.04972
2	σ_t	1.4094+ 2	0.80575	0.47984	0.33692
	σ_s	1.1917+ 1	1.00337	1.02488	1.03892
	σ_γ	2.0587+ 1	0.72069	0.34714	0.21086
	σ_f	1.0844+ 2	0.80018	0.44514	0.28371
3	σ_t	1.6883+ 1	0.97519	0.87935	0.77751
	σ_s	1.0738+ 1	0.98784	0.92790	0.85192
	σ_γ	6.8708- 1	0.94311	0.74443	0.55303
	σ_f	5.3422+ 0	0.95151	0.78495	0.62758
4	σ_t	6.5712+ 0	0.99767	0.98878	0.97827
	σ_s	3.8421+ 0	0.99661	0.98367	0.96834
	σ_γ	1.4501- 2	0.98830	0.93794	0.87327
	σ_f	2.0142+ 0	1.00184	1.00893	1.01736

JEF-2.2	REACT	AVERAGES	σ_{50b}	$\frac{1}{\Phi}$	$\frac{1}{P_{gi}}$
1	σ_t	5.2153+ 3	0.74351	0.13496	0.05256
	σ_s	1.9711+ 1	0.90745	0.70844	0.67364
	σ_γ	4.1246+ 2	0.74367	0.13649	0.05360
	σ_f	4.7832+ 3	0.74282	0.13246	0.04991
2	σ_t	1.4224+ 2	0.80769	0.48066	0.33731
	σ_s	1.2684+ 1	0.99760	0.9905	0.98354
	σ_γ	2.0357+ 1	0.71969	0.34382	0.20948
	σ_f	1.0920+ 2	0.80204	0.44694	0.28608
3	σ_t	1.5764+ 1	0.97508	0.87804	0.77387
	σ_s	9.4459+ 0	0.98915	0.93190	0.85681
	σ_γ	6.1593- 1	0.94615	0.75795	0.57361
	σ_f	5.5448+ 0	0.95124	0.78152	0.61795
4	σ_t	6.4042+ 0	0.99815	0.99130	0.98338
	σ_s	3.4254+ 0	0.99765	0.98890	0.97867
	σ_γ	2.0176- 2	0.99113	0.95517	0.91050
	σ_f	2.0933+ 0	1.00260	1.01247	1.02416

JENDL-3	REACT	AVERAGES	σ_{50b}	$\frac{1}{\Phi}$	$\frac{1}{P_{gi}}$
1	σ_t	5.3091+ 3	0.74316	0.13330	0.05174
	σ_s	1.6215+ 1	0.91139	0.74133	0.72039
	σ_γ	4.0483+ 2	0.74378	0.13705	0.05549
	σ_f	4.8880+ 3	0.74255	0.13098	0.04921
2	σ_t	1.4428+ 2	0.80795	0.45291	0.29113
	σ_s	1.1927+ 1	0.99961	1.00613	1.00647
	σ_γ	2.0974+ 1	0.73232	0.33057	0.17448
	σ_f	1.1138+ 2	0.80166	0.41670	0.23649
3	σ_t	1.6584+ 1	0.97439	0.87869	0.77862
	σ_s	1.0623+ 1	0.98678	0.92464	0.84728
	σ_γ	5.5805- 1	0.94507	0.76020	0.58562
	σ_f	5.2823+ 0	0.94995	0.78288	0.62732
4	σ_t	6.7298+ 0	0.99813	0.99109	0.98278
	σ_s	3.6668+ 0	0.99756	0.98835	0.97745
	σ_γ	2.0031- 2	0.98854	0.94072	0.88011
	σ_f	2.1141+ 0	1.00191	1.00923	1.01797

Table 3.7: Average cross section values for U^{233}

ENDF/B-VI	σ_{2200}	$\bar{\sigma}$	I_R	σ_{fiss}
σ_t	5.87846E+02	5.2302E+02	1.02887E+03	7.49673E+00
σ_s	1.27433E+01	1.2505E+01	1.45071E+02	4.61689E+00
σ_{in}	0.00000E+00	0.0000E+00	8.26873E-02	9.36325E-01
σ_f	5.29268E+02	4.6872E+02	7.47284E+02	1.89266E+00
σ_γ	4.58351E+01	4.1797E+01	1.36434E+02	4.71271E-02
JEF-2.2	σ_{2200}	$\bar{\sigma}$	I_R	σ_{fiss}
σ_t	5.86466E+02	5.2197E+02	1.03028E+03	7.13452E+00
σ_s	1.45666E+01	1.4288E+01	1.42099E+02	4.06005E+00
σ_{in}	0.00000E+00	0.0000E+00	1.49644E-01	1.18920E+00
σ_f	5.25924E+02	4.6576E+02	7.53570E+02	1.82471E+00
σ_γ	4.59753E+01	4.1924E+01	1.34461E+02	5.47017E-02
JENDL-3	σ_{2200}	$\bar{\sigma}$	I_R	σ_{fiss}
σ_t	5.91569E+02	5.2574E+02	1.04820E+03	7.51752E+00
σ_s	1.20259E+01	1.2001E+01	1.44576E+02	4.26753E+00
σ_{in}	0.00000E+00	0.0000E+00	6.38672E-02	1.24818E+00
σ_f	5.34044E+02	4.7212E+02	7.65340E+02	1.93476E+00
σ_γ	4.54992E+01	4.1619E+01	1.38220E+02	6.44064E-02

3.3.5 Runtime and Size of ENDF tapes

It is clear that the computer time and disk space required to process a material is an important aspect of the usability of a calculational path. The sizes of the ENDF tapes and the time required to process them with the NJOY program is given in Table 3.10. The first column in the table gives the size of the ENDF tape, the second column gives the total elapsed time as reported by NJOY and the last column gives the required disk space to process the evaluation including intermediate tapes and scratch files. There are differences up to a factor of two for the run time and disk space requirements between ENDF tapes. The longest run time is for JEF-2.2 U^{235} with 4166 seconds (1.15 hours) while the shortest one is for JEF-2.2 U^{233} with 331 seconds (5.5 minutes).

Table 3.8: 4 Group Cross Sections for Th^{232}

ENDF/B-VI	REACT	AVERAGES	σ_{50b}	$\frac{1}{\phi}$	$\frac{1}{P_{sl}}$
1	σ_t	8.5722+ 1	0.80030	0.37509	0.24356
	σ_s	1.7583+ 1	0.92058	0.77821	0.74259
	σ_γ	6.8139+ 1	0.76926	0.27107	0.11478
2	σ_t	3.1554+ 1	0.47132	0.39116	0.36673
	σ_s	1.9425+ 1	0.65328	0.59373	0.56443
	σ_γ	1.2128+ 1	0.17987	0.06669	0.05009
3	σ_t	1.5913+ 1	0.86780	0.78509	0.71130
	σ_s	1.4452+ 1	0.88614	0.80669	0.72720
	σ_γ	1.2113+ 0	0.60929	0.41089	0.32331
4	σ_t	6.5277+ 0	0.99728	0.98682	0.97440
	σ_s	3.4757+ 0	0.99602	0.98070	0.96254
	σ_γ	3.3711- 2	0.98128	0.90512	0.81125
	σ_f	2.9946- 1	1.01325	1.06494	1.12668
JEF-2.2	REACT	AVERAGES	σ_{50b}	$\frac{1}{\phi}$	$\frac{1}{P_{sl}}$
1	σ_t	8.4028+ 1	0.97949	0.36187	0.23133
	σ_s	1.6071+ 1	0.92032	0.77844	0.74481
	σ_γ	6.7957+ 1	0.76733	0.26336	0.10990
2	σ_t	2.8857+ 1	0.43493	0.34431	0.30977
	σ_s	1.6791+ 1	0.62762	0.55252	0.50300
	σ_γ	1.2067+ 1	0.16680	0.05459	0.04088
3	σ_t	1.3927+ 1	0.86333	0.78293	0.70552
	σ_s	1.2417+ 1	0.88488	0.80819	0.72399
	σ_γ	1.2018+ 0	0.59326	0.40130	0.32213
4	σ_t	6.3904+ 0	0.99801	0.99070	0.98224
	σ_s	3.7143+ 0	0.99700	0.98574	0.97251
	σ_γ	3.7698- 2	0.99104	0.95242	0.90251
	σ_f	2.8975- 1	1.00953	1.04645	1.09074
JENDL-3	REACT	AVERAGES	σ_{50b}	$\frac{1}{\phi}$	$\frac{1}{P_{sl}}$
1	σ_t	8.6771+ 1	0.80301	0.38498	0.25289
	σ_s	1.8637+ 1	0.92135	0.78130	0.74598
	σ_γ	6.8134+ 1	0.77064	0.27657	0.11801
2	σ_t	3.2183+ 1	0.47975	0.39716	0.36329
	σ_s	2.0169+ 1	0.66156	0.59766	0.55268
	σ_γ	1.2014+ 1	0.17455	0.06057	0.04535
3	σ_t	1.6113+ 1	0.88719	0.80515	0.72777
	σ_s	1.4717+ 1	0.90372	0.82378	0.74017
	σ_γ	1.0916+ 0	0.61637	0.40552	0.30314
4	σ_t	6.6902+ 0	0.99833	0.99172	0.98357
	σ_s	3.5265+ 0	0.99768	0.98815	0.97611
	σ_γ	3.1181- 2	0.98801	0.93788	0.87406
	σ_f	3.1007- 1	1.00784	1.03776	1.07316

Table 3.9: Average cross section values for Th^{232}

ENDF/B-VI	σ_{2200}	$\overline{\sigma}$	I_R	σ_{fiss}
σ_t	2.04362E+01	1.9589E+01	3.03505E+02	7.53049E+00
σ_s	1.30231E+01	1.3017E+01	2.18033E+02	4.49789E+00
σ_{in}	0.00000E+00	0.0000E+00	3.09057E-02	2.85926E+00
σ_f	0.00000E+00	0.0000E+00	0.00000E+00	7.69388E-02
σ_γ	7.41309E+00	6.5722E+00	8.54411E+01	8.68805E-02
JEF-2.2	σ_{2200}	$\overline{\sigma}$	I_R	σ_{fiss}
σ_t	1.93462E+01	1.8483E+01	2.72683E+02	7.12964E+00
σ_s	1.19347E+01	1.1930E+01	1.87577E+02	4.61205E+00
σ_{in}	0.00000E+00	0.0000E+00	2.00945E-01	2.33980E+00
σ_f	0.00000E+00	0.0000E+00	0.00000E+00	7.32254E-02
σ_γ	7.41145E+00	6.5536E+00	8.49075E+01	9.44324E-02
JENDL-3	σ_{2200}	$\overline{\sigma}$	I_R	σ_{fiss}
σ_t	2.12665E+01	2.0410E+01	3.08985E+02	7.47878E+00
σ_s	1.38346E+01	1.3830E+01	2.24983E+02	4.30609E+00
σ_{in}	0.00000E+00	0.0000E+00	1.76261E-01	3.00208E+00
σ_f	0.00000E+00	0.0000E+00	0.00000E+00	8.04975E-02
σ_γ	7.43200E+00	6.5798E+00	8.38265E+01	8.12711E-02

Table 3.10: CPU time and Disk Space requirements for NJOY

U^{238}	ENDF size (KByte)	run time (sec)	disk req. (MB)
ENDF/B-VI	602.6	3665.0	50
JEF-2.2	646.0	3353.0	50
JENDL-3	652.2	1936.8	35
U^{235}	ENDF size (KByte)	run time (sec)	disk req. (MB)
ENDF/B-VI	1240.0	4118.0	85
JEF-2.2	1230.0	4166.0	85
JENDL-3	546.0	2700.0	40
Th^{232}	ENDF size (KByte)	run time (sec)	disk req. (MB)
ENDF/B-VI	374.0	926.7	15
JEF-2.2	113.0	702.0	10
JENDL-3	235.3	942.0	15
U^{233}	ENDF size (KByte)	run time (sec)	disk req. (MB)
ENDF/B-VI	205.0	539.2	15
JEF-2.2	361.0	331.0	15
JENDL-3	328.0	676.8	25

Chapter 4

Benchmark Problems

The Cross Section Evaluation Working Group (CSEWG) is responsible for the generation and publication of "benchmark" problems which can be used to compare calculated values with experimental cross section parameters. The following benchmark problems from the CSEWG suite were used to perform the study.

4.1 TRX-1 and TRX-2

These benchmarks are H_2O moderated lattices of 1.3 % enriched uranium metal rods with 0.4915cm diameter arranged in a triangular pattern. The physical properties of the lattice are given in Table 4.1. These lattices directly test the U^{235} resonance fission integral and the thermal fission cross section . The U^{238} shielded resonance capture and the thermal capture cross section are also tested.

The analysis of the TRX lattices is made via a heterogeneous infinite cell calculation using the S_4 method followed by a homogenized core leakage calculation.

The WIMS input used to model the lattices is given in Appendix C.1.

The experimental data for these lattices are given in Table 4.2. Values in

Table 4.1: Physical Properties of the TRX-1 and TRX-2 lattices.

Region	Outer Radius, cm	Isotope	Concentration 10^{24} Atoms/cm^3
Fuel	0.4915	U^{235} U^{238}	6.253×10^{-4} 4.7205×10^{-2}
Void	0.5042	-	-
Clad	0.5753	Al	6.025×10^{-2}
Moderator	1.806 (TRX1) 2.174 (TRX2)	H^1 O^{16}	6.676×10^{-2} 3.338×10^{-2}

Table 4.2: Experimental data for TRX-1 and TRX-2 lattices.

	TRX-1	TRX-2
Pitch (cm)	1.8060	2.1740
Water/fuel vol. ratio	2.35	4.02
Number of rods	764	578
B^2 (10^{-4}cm^{-2})	57 (1)	54.69 (.36)
ρ^{28}	1.320 (.021)	0.837 (.016)
δ^{25}	0.0987 (.001)	0.0614 (.0008)
δ^{28}	0.0946 (.0041)	0.0693 (.0035)
C*	0.797 (.008)	0.647 (.006)

parenthesis are experimental uncertainties. The experimental parameters correspond to a thermal cutoff of 0.625 eV and are measured at the core center and their description is given below.

ρ^{28} the ratio of epithermal to thermal U^{238}captures.

δ^{25} the ratio of epithermal to thermal U^{235} fissions.

δ^{28} the ratio of U^{238} fissions to U^{235} fissions.

C* the ratio of U^{238} captures to U^{235} fissions (the conversion ratio).

These parameters depend on the spectrum and the particular isotope microscopic cross-sections. The difference between the calculated and measured value for each of these parameters gives an indication on the performance of the multigroup library.

Table 4.3: Physical Properties of the BAPL-1, BAPL-2 and BAPL-3 lattices.

Region	Outer Radius, cm	Isotope	Concentration 10^{24} Atoms/cm^3
Fuel	0.4864	U^{235}	3.112×10^{-4}
		U^{238}	2.3127×10^{-2}
		O	4.6948×10^{-2}
Void	0.5042	-	-
Clad	0.5753	Al	6.025×10^{-2}
Moderator	1.5578, 1.6523	H^1	6.676×10^{-2}
	and 1.8057 resp.	O^{16}	3.338×10^{-2}

Table 4.4: Experimental data for the BAPL lattices.

	BAPL-1	BAPL-2	BAPL-3
Pitch (cm)	1.5578	1.6523	1.8057
Water/fuel vol. ratio	1.43	1.78	2.40
Number of rods	2173 (3)	1755 (3)	1575 (3)
B^2 (10^{-4}cm^{-2})	32.59 (.15)	35.47 (.15)	34.22 (.13)
ρ^{28}	1.39 (.01)	1.12 (.01)	0.906 (.01)
δ^{25}	0.084 (.002)	0.068 (.001)	0.052 (.001)
δ^{28}	0.078 (.004)	0.070 (.004)	0.057 (.003)

4.2 BAPL-1, BAPL-2 and BAPL-3

These are H_2O moderated critical lattices with 1.311 % enriched uranium oxide of 0.9728 cm outer diameter which are arranged in a triangular pattern. The measured parameters are ρ^{28}, δ^{25}, δ^{28} and B^2. The physical properties of the lattices are given in Table 4.3. The WIMS input used to model this lattices is given in Appendix C.2.

The experimental results for the various parameters are given in table 4.4. Experimental uncertainties are given in parenthesis. The measured parameters correspond to a thermal cutoff of 0.625 eV and are measured at core center.

4.3 BNL-1, BNL-2 and BNL-3

There is very limited data on Th^{232}-U^{233} fueled nuclear benchmark lattices. The reference problems available in the CSEWG are the BNL-1, BNL-2 and BNL-3 lattices. These are used to study the performance of the ENDF libraries in a Th^{232}-U^{233} fueled system. The experimental data of these lattices are limited to the ratio of epithermal to thermal captures in Th^{232} (ρ^{02}) and the Dysproposium-164 disadvantage factor which is actually the ratio of the activations of Dy^{164} in the moderator to those in the fuel.

These lattices are H_2O moderated exponential lattices fueled by 3 % $^{233}UO_2$ and 97 % ThO_2. The fuel rods, which have an outer diameter of 1.0922cm, have a Zircaloy-2 clad and are arranged in a triangular pattern in a 180 cm diameter to 180 cm deep aluminum tank erected on top of a thermal column. The fuel to water ratio of the lattices are 1.0, 1.38 and 3.0 respectively. These lattices are sensitive to cross sections for thermal and epithermal U^{233} fission, thermal and epithermal Th^{232} capture, and H_2O scattering.

The physical properties of these lattices are given in Table 4.5 The experimental data for these lattices are given in Table 4.6. The experimental uncertainty for each value is given in parenthesis.

The analysis of these lattices is made (as in the previous lattices) via a heterogeneous infinite cell calculation followed by a homogenized core leakage calculation. The WIMS input used to model the lattices is given in Appendix C.3.

As stated before the experimental values of the BNL lattices are restricted to ρ^{02} and k_{eff}. In order to compare the results the following parameters are calculated.

ρ^{02} the ratio of epithermal to thermal captures in Th^{232}

δ^{23} the ratio of epithermal to thermal fissions in U^{233}.

Table 4.5: Physical Properties of the BNL-1,BNL-2 and BNL-3 lattices

Region	Outer Radius, cm	Isotope	Concentration 10^{24} Atoms/cm^3
Fuel	0.5462	Th^{232}	1.9811×10^{-2}
		U^{233}	6.1021×10^{-4}
		O	4.088×10^{-2}
Clad	0.6337	Zircaloy-2	4.4355×10^{-2}
Moderator	1.5923, 1.7188	H^1	6.676×10^{-2}
	and 2.1697 resp.	O^{16}	3.338×10^{-2}

Table 4.6: Experimental data for the BNL lattices.

	BNL-1	BNL-2	BNL-3
Pitch (cm)	1.5923	1.7188	2.1697
Water/fuel vol. ratio	.997	1.384	3.0043
Number of rods	511	397	271
B^2 (10^{-4}cm^{-2})	75.88 (2.0)	86.06 (1.3)	85.54 (0.8)
ρ^{02}	1.338 (.042)	.903 (.038)	.421 (.013)
δ_{Dy}	1.219 (.024)	1.257 (.024)	1.325 (.024)

δ_{23}^{02} the ration of Th^{232} fissions to U^{233} fissions.

C* the ratio of captures in Th^{232} to U^{233}.

4.4 Processing Considerations

4.4.1 Materials and Methods

The materials processed in order to produce the multigroup WIMS-D4 library are shown in Table 4.7. Figure 3.1 gives the overall calculational flow path that is used to process the materials with NJOY. After the conversion of the data to binary form RECONR is used to reconstruct resonance cross sections from resonance parameters. The reconstruction tolerance is set by an fractional error parameter which is given by the user in the input file.

A lower fractional (say 1%) error means better reconstruction but uses much more CPU time and disk space. The fractional error for all materials is given as 5% for our cases. The module BROADR uses the output RECONR tape to generate Doppler-broadened cross sections using the "kernel broadening method'.

UNRESR is used to produce effective self-shielded cross sections for resonance reactions in the unresolved energy range. The resonance information for the unresolved range is given as average values for resonance widths. This representation is converted into effective cross sections using the Bondarenko method.

The pointwise neutron scattering cross sections in the thermal range are generated by the THERMR module of NJOY. Inealistic cross sections and transfer matrices can be produced for a gas of free atoms, or for bound scatterers when ENDF $S(\alpha,\beta)$ scattering functions are available. The free gas approximation is used for all materials except Hydrogen since only that material had the necessary $S(\alpha,\beta)$ data from ENDF/B-VI.

The multigroup cross sections are produced by the GROUPR module with the use of the Bondarenko narrow-resonance weighting scheme. The Bondarenko σ_0 is chosen to represent the total mixture cross section for materials that are in position of the major resonance absorber. Smaller σ_0 values are used for isotopes that have relatively narrow resonances spaced relatively widely, such as U^{238} while for materials with stronger overlap, such as U^{235} a higher value is more reasonable.

Optionally, a weighting flux can be computed for various mixtures of heavy absorbers with light moderators (flux calculator option). An accurate pointwise solution of the integral slowing down equation is used. This option is normally called on to account for intermediate resonance effects in the epithermal range (8). In this study the flux calculator is used by assuming an infinite homogeneous mixture of U^{238} and Hydrogen for the TRX and BAPL lattices and an infinite homogeneous mixture

Table 4.7: Material numbers of the nuclides processed from the data libraries

Material	WIMS-D4	ENDF/B-6, JEF and JENDL
U^{238}	2238.4	9237.1
U^{235}	235.4	9228.1
U^{233}	9233.1	9222.1
Th^{232}	2232.1	9040.1
Zircaloy-2	91	—
Al^{27}	27	1325
O^{16}	16	825
H^2	2001	125
H_2O	—	1

of Th^{232} and Hydrogen for the BNL lattices.

There are two approaches to the averaging flux used in generating the WIMS-D4 multigroup library.

1. The built in EPRI-CELL spectrum for all materials which is typical for light water reactors.

2. Build in EPRI-CELL LWR spectrum with flux calculator for U^{238}. The generated flux is written to a file and used as input for U^{235}.

The first one is the classical approach which is often used to generate multigroup libraries for thermal systems. The second approach is used to get an approximate correction for resonance-resonance interference. Both methods are used in order to get a view of the effect of the second approach to the benchmark problems.

The Th^{232}-U^{233} fueled BNL benchmarks are also processed similarly.

The fission spectrum used in the generated WIMS library is taken from the original WIMS library. This assumption has little effect on the effective multiplication

factor but must be taken into account in the δ^{28} parameter for the TRX and BAPL lattices and the δ_{23}^{02} parameter for the BNL lattices.

The processing details for each material are as follows :

Uranium-238 : For U^{238} the data is generated at 300, 600 and 900 K. The self shielded cross sections are calculated for ten σ_0 values of 1.E10, 1.E4, 3.6E3, 1.E3, 2.613E2, 1.46E2, 65.34, 31.49, 15.53 and 1.0 barn. The reference σ_0 used in WIMSR is 65.34 barn. The flux calculator case is computed for a homogenous mixture of uranium and hydrogen in an infinite medium.The break between computed flux and bondarenko flux is taken as 347.87 eV. The NJOY input to process U^{238} is given in Appendix B.1.

Uranium-235 : The data is tabulated at 300, 600, and 900 K and the σ_0 values are taken as 1.E10, 1.E4, 3.6E3, 1.E3, 2.613E2, 1.46E2, 65.34, 31.49, and 15.5 barn. The reference σ_0 in WIMSR is 1.E10 which corresponds to infinite medium σ_0. The input used in NJOY for U^{235} is given in Appendix B.2.

Thorium-232 : The data for Th^{232} is generated at 300, 600 and 900 K. and the σ_0 values are 1.E10, 1.E4, 3.E3, 1.E3, 8.E2, 4.E2, 1.E2, 5.E1, 1.E1 and 1.0 barn. The flux calculator for a homogenous mixture of Th^{232} and Hydrogen in infinite medium. The Appendix B.4 lists the NJOY input for Th^{232}.

Uranium-233 : The data is tabulated at 300, 600 and 900 K and the σ_0 values are 1.E10, 1.E4, 3.6E3, 1.E3, 8E2, 4E2, 100, 31.49, 15.53 and 1.0 barn. The NJOY input for U^{233} is given in Appendix B.3. The reference σ_0 in WIMSR is given as 1.E10.

Zircaloy-2 : No processing is made for Zircaloy-2. The data is taken from the WIMS library.

Aluminum : All group constants are generated at 300 K. Since the sensitivity of the integral results to aluminum data is very low (10) no special assumptions are made while producing multigroup cross sections. The input used for Aluminum is listed in Appendix B.5.

Oxygen : The group constants for oxygen are calculated at 300 K except P1 matrices. The P1 scattering matrices are taken explicitly from the original WIMS library so there are no corrections to the self-scattering terms of the scattering matrix. The input to process Oxygen is given in Appendix B.6.

Hydrogen bound in Water : The hydrogen data is fully taken from the ENDF/B-VI library. A temperature of 300 K is used to calculate the group constants. The P1 matrix for Hydrogen (i.e. Thermal scattering data) bound in water is generated from ENDF/B-VI. This data is actually an evaluation produced at General Atomic in 1969 using the GASKET code. The only changes made to the contents in ENDF/B-VI are adjustments of cross sections to match the ENDF/B-VI values. The NJOY input to generate the data is given in Appendix B.7

4.4.2 Resonance Integral and Cross Sections

The resonance integrals in WIMS are specified for absorption and neutron yield per fission (i.e. the product of the average number of neutrons per fission and the fission cross section) (10) for resonant materials. These parameters are tabulated as a function of the background cross section σ_b. The equation

$$\sigma_b = \sigma_0 + \lambda\sigma_p \tag{4.1}$$

gives the relationship between the Bondarenko σ_0 and σ_b. Here λ is the

Goldstein-Cohen parameter and σ_p is the potential scattering cross section of the absorber. Since σ_p is the contribution of the absorber scattering it is more reasonable to use the shielded elastic cross section in place of a constant σ_p value. Additionally the self-shielding data is expressed in the WIMS code in terms of "resonance integrals", instead of using the self-shielded cross sections produced by GROUPR.

The results are not very sensitive to the definition of σ_p as the shielded elastic cross section as long as the definiton of the resonance integral is consistent. That is,

$$\sigma_x(\sigma_0) = \frac{\sigma_P I_x(\sigma_P)}{\sigma_P - I_a(\sigma_P)}\,, \tag{4.2}$$

and

$$I_x(\sigma_P) = \frac{\sigma_P \sigma_x(\sigma_0)}{\sigma_P + \sigma_a(\sigma_0)}\,, \tag{4.3}$$

where x denotes the reaction and I_x is the corresponding resonance integral.

The Goldstein Cohen parameter is applied as 0.188 for U^{238}, 0.1965 for U^{235}, 0.1965 for Th^{232} and 0.2 for U^{233}. This parameters are taken from the original WIMS library.

There is no processing of burnup data and fission product yields for the materials.

Chapter 5

Results and Conclusion

In order to verify the approach used in generating the multigroup group constants the results of the WIMS calculations for the selected benchmarks using the newly generated library generated from ENDF/B-VI, JEF-2.2 and JENDL-3 are compared with the published reference results.

A sensitivity analysis investigating the effect of U^{238} and Hydrogen to the benchmark parameters is made for the TRX and BAPL lattices.

There are actually two sets of ENDF results differing from their approach of treating the weighting flux for U^{235} (U^{233} for BNL). In the first set, (i.e. ENDF/B-VI (1) etc.) the weighting flux is taken as EPRI-CPM while in the second set (ENDF/B-VI (2) etc.) the weighting flux is from the U^{238} (e.g. Th^{232} for BNL lattices) flux calculation.

Additionally the effect of the fission spectrum to the benchmark parameters is analyzed for the BNL lattices.

5.1 Sensitivity of TRX and BAPL lattices to U^{238} and Hydrogen

The approach to investigate the effect of U^{238} and Hydrogen to the benchmark parameters is to replace U^{238} and Hydrogen processed from ENDF/B-VI in place

of the WIMS library U^{238} and Hydrogen.

The results for the analysis are given in Table 5.1. The effect of U^{238} is to decrease k_{eff} for as much as 2 % for the TRX lattices and 1.5 % for the BAPL lattices. The ratio of the epithermal to thermal capture reaction rate in U^{238} (ρ^{28}) increased approximately between 8 % for the TRX cases and 5 % for the BAPL cases. The conversion ratio is also increased for approximately 5 % in all lattices. The improvement in the ρ^{28} values show that the treatment of U^{238} in the ENDF/B-VI processes is better than in the original WIMS library.

The effect of Hydrogen is smaller but not negligible. The ENDF/B-VI processed Hydrogen (which has a new P1 scattering matrix) increases k_{eff} for 0.5 % in the TRX cases and 0.6 % in the BAPL cases. ρ^{28} is decreased for approximately 1 % in all lattices. Obviously the effect of ENDF/B-VI processed U^{238} and Hydrogen is opposite to each other and will cancel out for a specific amount if simultaneously used in a problem (as is done in the next sections).

5.2 TRX-1 and TRX-2

Tables 5.2 and 5.3 summarizes the results obtained from the TRX-1 and TRX-2 lattices.

The effective multiplication factor (k_{eff}) is underpredicted for all the cases except WIMS-D4 and is outside the experimental uncertainty which is 0.30 % for TRX-1 and 0.10 % for TRX-2. It is observed that the effect of the flux-calculator to k_{eff} is tp decrease k_{eff} for further 0.1 % to 0.2 %. This situation arises because of the different weighting flux applied for U^{235} in this case. The closest result to the experimental value is that of JENDL-3(1) for both lattices. Since it is shown in Section 3.3.4 that the U^{238} data for JEF and ENDF/B is principally the same it can be deduced that the difference observed in k_{eff} and the other benchmark parameters for these two

Table 5.1: Sensitivity of TRX and BAPL lattices to H and U^{238}

TRX-1	k_{eff}	ρ^{28}	δ^{25}	δ^{28}	CR
Measured	1.0000	1.320	0.0987	0.0946	0.797
WIMS-D4	1.0002	1.272	0.0996	0.0963	0.777
H	1.0047	1.258	0.0991	0.0945	0.774
U238	0.9755	1.361	0.0100	0.0971	0.824
TRX-2	k_{eff}	ρ^{28}	δ^{25}	δ^{28}	CR
Measured	1.0000	0.837	0.0614	0.0693	0.647
WIMS-D4	0.9953	0.801	0.0612	0.0691	0.633
H	0.9995	0.792	0.0610	0.0679	0.631
U238	0.9784	0.851	0.0618	0.0686	0.664
BAPL-1	k_{eff}	ρ^{28}	δ^{25}	δ^{28}	CR
Measured	1.0000	1.390	0.0840	0.0780	–
WIMS-D4	1.0020	1.349	0.0842	0.0755	0.797
H	1.0053	1.336	0.0792	0.0741	0.794
U238	0.9809	1.417	0.0850	0.0753	0.837
BAPL-2	k_{eff}	ρ^{28}	δ^{25}	δ^{28}	CR
Measured	1.0000	1.120	0.0680	0.0700	–
WIMS-D4	0.9972	1.125	0.0688	0.0651	0.729
H	1.0033	1.113	0.0684	0.0637	0.726
U238	0.9816	1.177	0.0693	0.0691	0.762
BAPL-3	k_{eff}	ρ^{28}	δ^{25}	δ^{28}	CR
Measured	1.0000	0.906	0.0520	0.0570	–
WIMS-D4	0.9976	0.886	0.0529	0.0536	0.654
H	1.0032	0.876	0.0526	0.0524	0.652
U238	0.9854	0.924	0.0533	0.0527	0.681

Table 5.2: Summary of benchmark parameters for TRX-1

TRX-1	k_{eff}	ρ^{28}	δ^{25}	δ^{28}	CR
MEASURED	1.0000	1.3200	0.0987	0.0946	0.797
WIMS-D4	1.0002	1.2725	0.0996	0.0963	0.777
ENDF/B-VI(1)	0.9887	1.3626	0.0979	0.0943	0.809
ENDF/B-VI(2)	0.9875	1, 3576	0.0983	0.0945	0.811
JEF-2.2 (1)	0.9902	1.3584	0.0980	0.0932	0.811
JEF-2.2 (2)	0.9890	1.3538	0.0981	0.0933	0.813
JENDL-3 (1)	0.9913	1.3555	0.0974	0.0933	0.809
JENDL-3 (2)	0.9900	1.3505	0.0975	0.0934	0.811

evaluations comes from the different treatment of U^{235}.

The results for the ratio of the epithermal to thermal capture reaction rates in U^{238} (ρ^{28}) are very close to the experimental error range which is 1.6 % for TRX-1 and 1.9 % for TRX-2 0. It is seen that the use of the flux calculator option improved (e.g. made it closer to the experimental value) this parameter for approximately 0.5 % in all cases. Although all values are close, JENDL-3 performed slightly better than ENDF/B and JEF.

The ratio of the epithermal to thermal fission reaction rates in U^{235} (δ^{25}) is in the experimental error range which is 1 % for TRX-1 and 1.3 % for TRX-2. The effect of the flux calculator flux for U^{235} is to make the parameter for about 0.25 % - 0.40 % closer to the experimental value in TRX-1. For TRX-2 the flux calculator decreased the parameter slightly in ENDF/B-VI while it increased it in JEF-2 and JENDL-3.

The ratio of the total fission reaction rates in U^{238} and U^{235} (δ^{28}) is again in the experimental error range which is 4.3 % for TRX-1 and 5.1 % for TRX-2. In TRX-1 ENDF/B-VI performed better with an improvement in the flux-calculator case which made it fairly close to the experimental value. For TRX-2 the results of the generated libraries are not as close to the experimental values as in TRX-1 but all lie in the experimental error range.

The ratio of the capture reaction rates in U^{238} and fission reaction rates in U^{235}, which actually is the conversion ratio (C*), are very close to or in the experimental error range of this parameter which is 1.0 % for TRX-1 and 0.93 % for TRX-2. The effect of the flux calculator flux for U^{235} is to increase the parameter for approximately 0.5 %. For both lattices WIMS-D4 calculated the conversion ratio outside the experimental error range.

Table 5.3: Summary of benchmark parameters for TRX-2

TRX-2	k_{eff}	ρ^{28}	δ^{25}	δ^{28}	CR
MEASURED	1.0000	0.8370	0.0614	0.0693	0.647
WIMS-D4	0.9953	0.8017	0.0612	0.0691	0.633
ENDF/B-VI(1)	0.9920	0.8516	0.0600	0.066	0.651
ENDF/B-VI(2)	0.9904	0.8485	0.0601	0.066	0.653
JEF-2.2 (1)	0.9928	0.8495	0.0602	0.066	0.654
JEF-2.2 (2)	0.9913	0.8566	0.0603	0.066	0.656
JENDL-3 (1)	0.9943	0.8481	0.0598	0.066	0.651
JENDL-3 (2)	0.9927	0.8450	0.0599	0.066	0.654

5.3 BAPL-1, BAPL-2 and BAPL-3

The results for the BAPL cases is shown in tables 5.4, 5.5 and 5.6. There is no experimental conversion ratio parameters for the BAPL lattices.

The effective multiplication factor is again underpredicted for the ENDF files and JENDL-3 (1) gives the closest results to the experimental value for all lattices. In BAPL-3 it even agrees 100 % with the experimental value. The error range is 0.1 % for all three lattices. The flux-calculator case again decreases the k_{eff} value by a small amount.

The ratio of the epithermal to thermal capture reaction rates in U^{238} (ρ^{28}), which has experimental error estimates of 0.72 % for BAPL-1, 0.89 % for BAPL-2 and 1.1 % for BAPL-3, is for the ENDF cases closer to the experimental value than the WIMS result. The closest results are again obtained with the JENDL-3 data (although the difference is very small). The flux calculator cases improved the accuracy slightly (about 0.3 % in the JENDL-3 case).

The ratio of the epithermal to thermal fission reaction rates in U^{235} (δ^{25}) is in the experimental error range which is 2.4 % for BAPL-1, 1.6 % for BAPL-2 and 1.9 % for BAPL-3. Despite the TRX lattices the effect of the flux calculator flux for U^{235} is

Table 5.4: Summary of benchmark parameters for BAPL-1

BAPL-1	k_{eff}	ρ^{28}	δ^{25}	δ^{28}	CR
MEASURED	1.0000	1.390	0.0840	0.0780	–
WIMS-D4	1.0020	1.349	0.0842	0.0754	0.797
ENDF/B-VI (1)	0.9928	1.429	0.0835	0.0729	0.824
ENDF/B-VI (2)	0.9912	1.423	0.0836	0.0730	0.824
JEF-2.2 (1)	0.9938	1.424	0.0836	0.0722	0.827
JEF-2.2 (2)	0.9924	1.419	0.0837	0.0723	0.829
JENDL-3 (1)	0.9950	1.422	0.0831	0.0725	0.824
JENDL-3 (2)	0.9935	1.417	0.0833	0.0726	0.827

Table 5.5: Summary of benchmark parameters for BAPL-2

BAPL-2	k_{eff}	ρ^{28}	δ^{25}	δ^{28}	CR
MEASURED	1.0000	1.120	0.0680	0.0700	–
WIMS-D4	0.9972	1.125	0.06881	0.0651	0.729
ENDF/B-VI (1)	0.9940	1.186	0.0689	0.0625	0.750
ENDF/B-VI (2)	0.9923	1.182	0.0681	0.0626	0.753
JEF-2.2 (1)	0.9949	1.183	0.0681	0.0621	0.753
JEF-2.2 (2)	0.9933	1.179	0.0682	0.0622	0.755
JENDL-3 (1)	0.9963	1.182	0.0677	0.0623	0.750
JENDL-3 (2)	0.9946	1.177	0.0678	0.0625	0.753

to change δ^{25} for a very small amount in all BAPL lattices. JEF-2.2 provided better results in BAPL-1 and BAPL-2 while JENDL-3 performed a little better in BAPL-3.

The ratio of the total fission reaction rates in U^{238} and U^{235} (δ^{28}) is not in the experimental error range which is 5.1 % for BAPL-1, 5.7 % for BAPL-2 and 5.3 % for BAPL-3 0. In BAPL-1 ENDF/B-VI performed better with an small increase in the flux-calculator case which made it fairly close to the experimental value.

Table 5.6: Summary of benchmark parameters for BAPL-3

BAPL-3	k_{eff}	ρ^{28}	δ^{25}	δ^{28}	CR
MEASURED	1.0000	0.906	0.0520	0.0570	–
WIMS-D4	0.9976	0.886	0.0529	0.0536	0.654
ENDF/B-VI (1)	0.9972	0.929	0.0521	0.0510	0.669
ENDF/B-VI (2)	0.9960	0.926	0.0522	0.0511	0.672
JEF-2.2 (1)	0.9984	0.927	0.0522	0.0508	0.672
JEF-2.2 (2)	0.9967	0.924	0.0523	0.0509	0.674
JENDL-3 (1)	1.0000	0.926	0.0519	0.0510	0.669
JENDL-3 (2)	0.9982	0.923	0.0520	0.0511	0.672

5.4 BNL-1, BNL-2 and BNL-3

The results for the ThO_2-U^{233} fueled BNL lattices are given in tables 5.7, 5.8 and 5.9. The experimental value of ρ^{02} is generally believed to be incorrect because of the failure to validate it via calculation.

JEF-2.2 performed quite well for the effective multiplication factor. The flux calculation case improved k_{eff} considerably. For ρ^{02} the ENDF/B-VI results are very close to the WIMS value of this parameter. The flux calculator case decreased the value of ρ^{02} slightly. For the ratio of epithermal to thermal fissions in U^{233} (δ^{23}) the values of JEF-2.2 and JENDL-3 are closer to the WIMS result. The ratio of Th^{232} fissions to U^{233} (δ^{02}_{23}) is consistent for all ENDF files with ENDF/B closer to the WIMS result. The effect of the flux calculator is rather small for this parameter. The conversion ratio (CR) is slightly increased in the flux calculator cases.

5.5 Effect on Fission Spectrum in the BNL Lattices

The calculations for the BNL lattices are repeated with three different U^{233} fission spectra. The first is the fission spectrum from ENDF/B-VI, the second is the fission spectrum from JEF-2.2 and the third is taken from JENDL-3. The graphical rep-

Table 5.7: Summary of benchmark parameters for BNL-1

BNL-1	k_{eff}	ρ^{02}	δ^{23}	δ_{23}^{02}	CR
MEASURED	1.0000	1.338	–	–	–
WIMS-D4	1.0025	1.162	0.5650	0.0146	0.614
ENDF/B-VI(1)	1.0176	1.153	0.5972	0.01422	0.600
ENDF/B-VI(2)	1.0167	1.150	0.5989	0.01423	0.601
JEF-2.2 (1)	1.0068	1.094	0.5586	0.01373	0.598
JEF-2.2 (2)	1.0060	1.091	0.5595	0.01374	0.599
JENDL-3 (1)	1.0300	1.056	0.5660	0.01456	0.578
JENDL-3 (2)	1.0282	1.053	0.5669	0.01458	0.579

Table 5.8: Summary of benchmark parameters for BNL-2

BNL-2	k_{eff}	ρ^{02}	δ^{23}	δ_{23}^{02}	CR
MEASURED	1.0000	0.903	–	–	–
WIMS-D4	1.0032	0.815	0.4069	0.0121	0.577
ENDF/B-VI(1)	1.0195	0.802	0.4297	0.0111	0.564
ENDF/B-VI(2)	1.0183	0.800	0.4310	0.0117	0.565
JEF-2.2 (1)	1.0095	0.765	0.4024	0.0113	0.563
JEF-2.2 (2)	1.0085	0.763	0.4031	0.0113	0.565
JENDL-3 (1)	1.0289	0.739	0.4075	0.0120	0.547
JENDL-3 (2)	1.0271	0.737	0.4082	0.0120	0.548

Table 5.9: Summary of benchmark parameters for BNL-3

BNL-3	k_{eff}	ρ^{02}	δ^{23}	δ_{23}^{02}	CR
MEASURED	1.0000	0.421	–	–	–
WIMS-D4	1.0086	0.386	0.1988	0.0078	0.522
ENDF/B-VI (1)	1.0273	0.374	0.2097	0.0075	0.512
ENDF/B-VI (2)	1.0255	0.372	0.2104	0.0075	0.514
JEF-2.2 (1)	1.0200	0.359	0.1969	0.0072	0.514
JEF-2.2 (2)	1.0191	0.358	0.1973	0.0072	0.515
JENDL-3 (1)	1.0319	0.348	0.1993	0.0078	0.502
JENDL-3 (2)	1.0299	0.347	0.1997	0.0078	0.504

resentation of the three spectra normalized with respect to the original WIMS fission spectrum is shown in Figure 5.1. The effect of the spectra to the benchmark parameters is given in Table 5.10. In the table the row with letter "a" in paranthesis gives the results for WIMS fission spectrum while the row with letter "b" in paranthesis gives the values for the alternative fission spectrum. The weighting flux used is EPRI-CPM for both Th^{232} and U^{233}.

The multiplication factor (k_{eff}) decreases for about 0.6 % in ENDF/B-VI calculations for the BNL lattices if the ENDF/B-VI spectra is used in place of the WIMS spectra. For JEF-2.2 calculation the decrease is smaller with 0.1 % - 0.15 % compared to calculations using WIMS spectra. The decrease for JENDL-3 calculations is approximately 0.55 % in all lattices. It can be seen from Figure 5.1 that the ENDF/B-VI and JENDL-3 spectra are close to each other while the JEF-2.2 spectra differs greatly from them. This explains why the decreases in k_{eff} in JENDL-3 and ENDF/B-VI are almost the same per-cent.

The differences for ρ^{02} are very small (less than 0.1%) for all lattices and all spectra. The same observation holds for δ^{23} too.

It can be concluded from these results that one should use the appropriate fission spectrum for the major fissile material of interest in the WIMS calculations.

5.6 Conclusion

The capability of processing materials from Evaluated Nuclear Data Files and generating multigroup libraries is powerful and important in many aspects. The Evaluated Nuclear Data Files have been very succesfull in providing a source of standardized and reliable nuclear data for a wide range of applications. A key component of processing the Evaluated Nuclear Data Files is data testing, which is important for finding errors and for giving the user an initial view of how well an

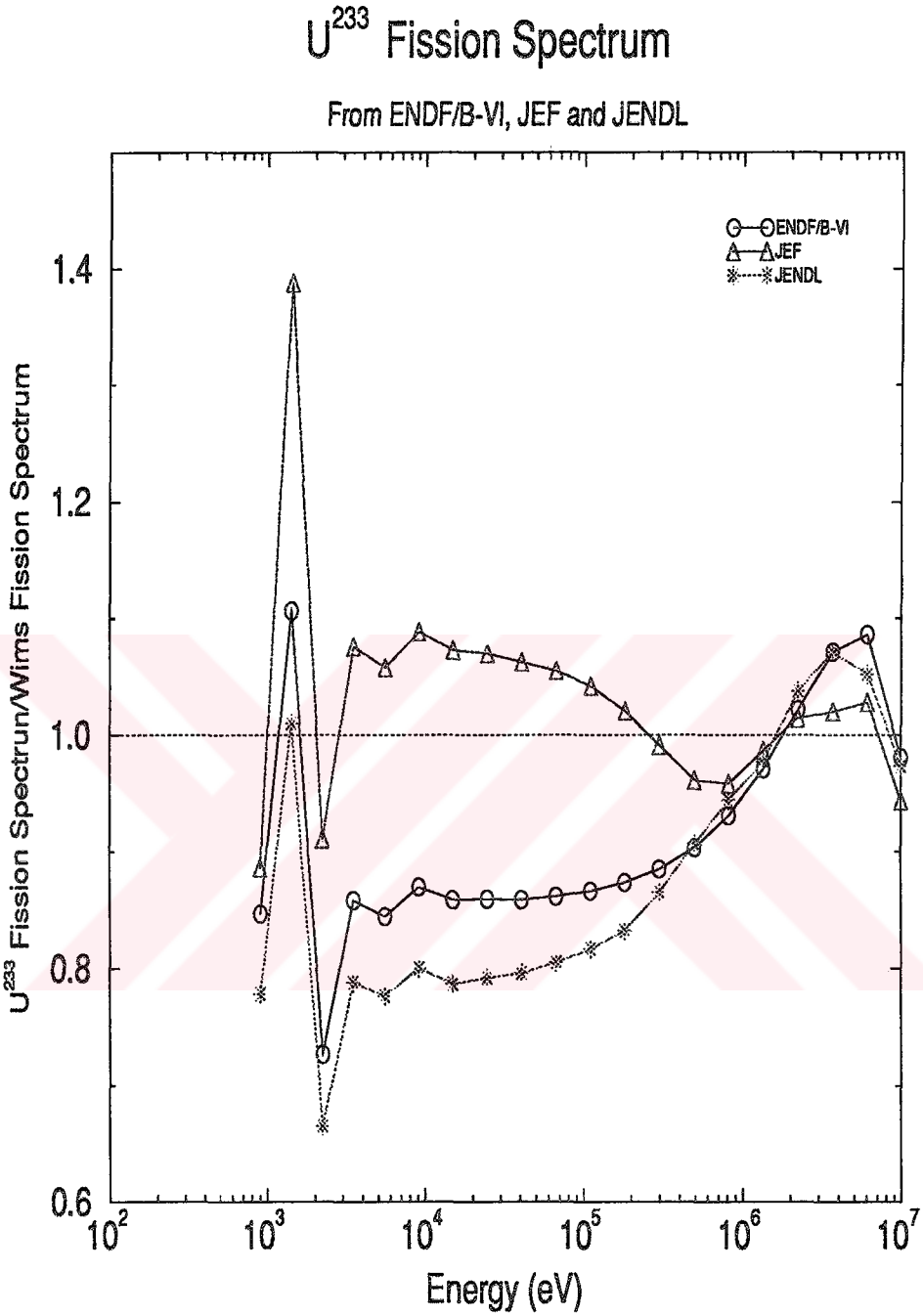

Figure 5.1: Normalized U^{233} Fission Spectra

Table 5.10: Results for different Fission Spectra

BNL-1	k_{eff}	ρ^{02}	δ^{23}	δ_{23}^{02}	CR
MEASURED	1.0000	1.338	–	–	–
WIMS-D4	1.0025	1.162	0.5650	0.0146	0.614
ENDF/B-VI(a)	1.0176	1.153	0.5972	0.0142	0.600
ENDF/B-VI(b)	1.0113	1.154	0.5978	0.0149	0.600
JEF-2.2 (a)	1.0068	1.094	0.5586	0.0137	0.598
JEF-2.2 (b)	1.0054	1.095	0.5587	0.0138	0.598
JENDL-3 (a)	1.0300	1.056	0.5660	0.0145	0.578
JENDL-3 (b)	1.0240	1.058	0.5666	0.0152	0.578
BNL-2	k_{eff}	ρ^{02}	δ^{23}	δ_{23}^{02}	CR
MEASURED	1.0000	0.903	–	–	–
WIMS-D4	1.0032	0.815	0.4069	0.0121	0.577
ENDF/B-VI(a)	1.0195	0.802	0.4297	0.0117	0.564
ENDF/B-VI(b)	1.0128	0.803	0.4301	0.0123	0.564
JEF-2.2 (a)	1.0095	0.765	0.4024	0.0113	0.563
JEF-2.2 (b)	1.0080	0.766	0.4025	0.0114	0.564
JENDL-3 (a)	1.0289	0.739	0.4075	0.0120	0.547
JENDL-3 (b)	1.0226	0.7408	0.4079	0.0126	0.547
BNL-3	k_{eff}	ρ^{02}	δ^{23}	δ_{23}^{02}	CR
MEASURED	1.0000	0.421	–	–	–
WIMS-D4	1.0086	0.386	.01988	0.0078	0.522
ENDF/B-VI (a)	1.0273	0.374	0.2097	0.0075	0.512
ENDF/B-VI (b)	1.0210	0.374	0.2099	0.0079	0.512
JEF-2.2 (a)	1.0200	0.359	0.1969	0.0072	0.514
JEF-2.2 (b)	1.0193	0.360	0.1970	0.0073	0.514
JENDL-3 (a)	1.0319	0.348	0.1993	0.0078	0.502
JENDL-3 (b)	1.0264	0.348	0.1995	0.0081	0.502

Evaluated Nuclear Data File and the multigroup library generated from it would be expected to perform in a problem. But using benchmark lattices to test Evaluated Nuclear Data Files is very difficult, and the results are often ambiguous. The difficulty is that very simple models have been specified for benchmarks which makes it easier for a large number of laboratories to compute the benchmarks. But this simplicity is also the source of the ambiguity (9). In many cases, model corrections are computed using previous data libraries and older methods. If a new calculation using a brand-new Evaluated Nuclear Data File gives worse answer than an old calculation it may not really prove that the new data doesn't perform better than the old one.

The evaluations for U^{238} in ENDF/B-VI and JEF-2.2 are principally the same which is evident from the cross sections generated by GROUPIE and validated with INTER in Section 3.3.4. The same observation is true for the U^{235} evaluations of ENDF/B-VI and JENDL which show only a small inconsistency in the fast range. The evaluations for U^{233} and Th^{232} appear to be different for all three ENDF files.

The use of the Hydrogen data from ENDF/B-VI in place of the original WIMS Hydrogen data increases k_{eff} while the use of ENDF/B-VI U^{238} instead of the WIMS U^{238} has the effect to decrease k_{eff} to a greater extent. The epithermal to thermal absorbtion in U^{238} (ρ^{02}) increased showing that the resonance treatment of the old WIMS library is different than that in ENDF/B-VI and explaining in part the decrease in k_{eff}. The results show that the absorbtion effect of ENDF/B U^{238} is always greater than the moderating effect of ENDF Hydrogen. There is an improvement in the reaction rates for the new multigroup data of U^{238} compared to the original WIMS library but there is overprediction in absorbtion. The effect of the new U^{235} is minor compared with U^{238}. The effect of the fluxcalculator flux for U^{235} is to increase the self shielding a bit. The new Th^{232} is generally less absorbing than the Th^{232} in the original WIMS

library.

The benchmark parameters except k_{eff} are generally closer to the experimental values for the ENDF libraries than for the original WIMS library for the TRX and BNL lattices.

The effect of using the U^{233} fission spectrum instead of the original WIMS fission spectrum in the BNL lattices is to decrease k_{eff} for JEF and ENDF/B for small amount while the decrease in JENDL is much larger. The reason for the larger decrease in JENDL is due to the fact that the fission spectrum from JENDL has generally a larger value than the fission spectrum from both JEF and ENDF. It is evident from the results that it is important to use the appropriate fission spectrum for the major fissile material of interest.

Data testing results like the ones reported in this work must be used cautiously. Clearly the "differences" between a new evaluation and old data is significant. If a researcher knows how calculations using the old data perform for its application, he can get, by examining the difference of the data, a pretty good idea of how the new evaluation will perform for the same application. This requires a thorough understanding of the problem by the researcher.

It is evident from the results that the use of a single evaluation may be not the best solution by itself but mixing the best performing materials into a single multigroup library is the best approach to get better results.

The following can be considered for future research :

Detailed analysis on using the ENDF/B-VI Hydrogen data can be made considering leakage effects and studying detailed reaction rate edits.

New Th^{232}-U^{233} cases with reliable experimental data can be found in order to study these type of problems more in detail.

The new 172 group WIMS structure and library for WIMS can be used and

the benchmark experiments repeated using this group structure. The finer group structure should give better indications on the performance of new evaluations than the 69 group structure used in this study.

Full scale sensitivity analysis can be done for all materials of interest in order to get a better understanding of the generated multigroup nuclear data.

The performance of the new evaluations in burnup calculations can be investigated by generating burnup data and performing burnup analysis.

Other codes than WIMS can be used to get a better view on the effect of the new evaluations without having to deal with WIMS specific code or library corrections.

The quality of the pointwise nuclear data can be investigated with the use of a Monte Carlo code like MCNP.

In summary, the results in these thesis show that there are some gains and some losses in using a new evaluation. The aim in using a new evaluation is to narrow the difference between reality and computational models. The researcher should consider the effect of the assumptions made in the calculational models to the new data. This is an important factor in getting a better understanding of the usability of the new data for the problem of interest.

It is up to the user to determine if the gains outweighs the losses, that means if generating a new multigroup library for his application is going to give better results or not.

References

(1) Y. Ronen, Ed., "Handbook of Nuclear Reactors Calculations" (CRC Press, Boca Raton, Florida, 1986).

(2) R. Kinsey, "ENDF-102, Data Formats and Procedures for the Evaluated Nuclear Data Files, ENDF," Brookhaven National Laboratory report BNL-NCS-50496 (ENDF 102) 2nd. Ed. (ENDF/B-V) (October 1979).

(3) H. D. Lemmel, Ed., "JEF-2 The Evaluated Nuclear Data Library of the NEA Data Bank" International Atomic Energy report IAEA-NDS-120 (1993).

(4) H. D. Lemmel, Ed., "JENDL-3, The Japanese Evaluated Nuclear Data Library" International Atomic Energy Agency report IAEA-NDS-110 (June 1990).

(5) D. E. Cullen, " The 1994 ENDF Pre-Processing Codes" International Atomic Energy Agency report NDS-39, Lawrence Livermore Nat. Lab. (1994).

(6) C. L. Dunford, "ENDF Utility Codes Fron NNDC, version 6.7" International Atomic Energy report NDS-29, National Nuclear Data Center (1991).

(7) D. E. Cullen, R. Muranaka, J. Schmidt, Ed., "Workshop on Reactor Physics Calculations for Applications in Nuclear Technology" (World Scientific Publishing Co., London, 1991)

(8) R. E. MacFarlane and D. W. Muir, "The NJOY Nuclear Data Processing System, Version 91," Los Alamos National Laboratory report LA-12740-M (to be published).

(9) R. E. MacFarlane, "Processing and Testing ENDF/B-VI with NJOY and TRANSX" Los Alamos National Laboratory (to be published).

(10) A. Trkov, M. Ravnik, "Application of ENDF/B-VI data for the WIMS Lattice Code" Annals of Nuclear Energy Vol. 20. No. 8, p. 561 (1993).

(11) R. E. MacFarlane, "ENDF/B-IV and -V Cross Sections for Thermal Power Reactor Analysis," in Proc. Intl. Conf. of Nuclear Cross Sections for Technology, Knoxville, TN (October 22-26 1979), National Bureau of Standards Publication 594 (September 1980).

(12) M. J. Roth, J. D. MacDougall, and P. B. Kemshell. "The Preparation of Input Data for WIMS" Technical Report AEEW-R 538, Atomic Energy Establishment, Winfrith, Dorchester, Dorset (1967).

Appendix A

Index of Evaluated Nuclear Data Files

The Index for the ENDF files is given patially in order to conderve space.

A.1 Index of the ENDF/B-VI Nuclear Data File

```
 1-H -  1 LANL       EVAL-OCT89 HALE, DODDER, SICILIANO, WILSON   125 1451    5
 1-H -  2 LANL,AWRE  EVAL-NOV67 L.STEWART (LASL) A.HORSLEY (AWRE) 128 1451    5
 1-T -  3 LANL       EVAL-FEB65 LEONA STEWART                    131 1451    5
 2-HE-  3 LANL       EVAL-MAY90 G.HALE, D.DODDER, P.YOUNG        225 1451    5
 2-HE-  4 LANL       EVAL-OCT73 NISLEY, HALE, YOUNG              228 1451    5
 3-LI - 6 LANL       EVAL-APR89 G.M.HALE, P.G.YOUNG              325 1451    5
 3-LI-  7 LANL       EVAL-AUG88 P.G.YOUNG                        328 1451    5
 4-BE-  9 LLNL       EVAL-JAN86 PERKINS, PLECHATY, HOWERTON      425 1451    5
 5-B - 10 LANL       EVAL-NOV89 G.M.HALE, P.G.YOUNG              525 1451    5
 5-B - 11 LANL       EVAL-MAY89 P.G.YOUNG                        528 1451    5
 6-C -  0 ORNL       EVAL-AUG89 C.Y.FU, E.J.AXTON AND F.G.PEREY  600 1451    5
 7- N- 14 LANL       EVAL-MAY90 P.YOUNG, G.HALE, M.CHADWICK      725 1451    5
 7- N- 15 LANL       EVAL-SEP83 E.ARTHUR,P.YOUNG,G.HALE          728 1451    5
 8-O - 16 LANL       EVAL-JAN90 G.HALE, Z.CHEN, P.YOUNG          825 1451    5
 8-O - 17 BNL        EVAL-JAN78 B.A.MAGURNO                      828 1451    5
 9-F - 19 CNDC,ORNL  EVAL-JUN90 Z.X.ZHAO,C.Y.FU,D.C.LARSON       925 1451    5
     ---------- Range Intentionally Deleted ----------
79-AU-197 LANL       EVAL-JAN84 P.G.YOUNG                      7925 1451    5
82-PB-206 ORNL       EVAL-MAR89 C.Y.FU,N.M.LARSON,D.C.LARSON   8231 1451    5
82-PB-207 ORNL       EVAL-MAR89 C.Y.FU,N.M.LARSON,D.C.LARSON   8234 1451    5
82-PB-208 ORNL       EVAL-MAR89 C.Y.FU, D.C.LARSON             8237 1451    5
82-BI-209 ANL        EVAL-AUG89 A.SMITH,D.SMITH,P.GUENTHER,    8325 1451    5
90-TH-230 HEDL       EVAL-NOV77 MANN                           9034 1451    5
```

```
90-TH-232 BNL,ANL+   EVAL-DEC77 BHAT,SMITH,LEONARD,DESAUSSURE+   9040 1451    5
91-PA-231 HEDL       EVAL-NOV77 MANN                              9131 1451    5
91-PA-233 GA,BNL,LANLEVAL-MAY78 MATHEWS,KINSEY,YOUNG              9137 1451    5
92-U -232 HEDL       EVAL-NOV77 MANN                              9219 1451    5
92-U -233 LANL,ORNL  EVAL-DEC78 STEWART ET AL, L. WESTON          9222 1451    5
92-U -234 BNL,GGA    EVAL-JUL78 DIVADEENAM,DRAKE,MANN+            9225 1451    5
92-U -235 ORNL,LANL  EVAL-NOV89 L.W.WESTON,P.G.YOUNG,W.P.POENITZ  9228 1451    5
92-U -236 HEDL       EVAL-OCT89 F.M. MANN, R.E. SCHENTER          9231 1451    5
92-U -237 BNL,SRL+   EVAL-JUL76 KINSEY-ASSEMBLER(SEE COMMENTS)   9234 1451    5
92-U -238 ORNL,LANL+ EVAL-NOV89 L.W.WESTON,P.G.YOUNG,W.POENITZ    9237 1451    5
93-NP-237 LANL       EVAL-APR90 P.YOUNG, E.ARTHUR, F.MANN         9346 1451    5
93-NP-238 SRL        EVAL-AUG75 BENJAMIN AND MCCROSSON            9349 1451    5
93-NP-239 ORNL       EVAL-DEC88 R. Q. WRIGHT                      9352 1451    5
94-PU-236 HEDL,SRL   EVAL-APR78 MANN,SCHENTER,BENJAMIN,MCCROSSON 9428 1451    5
94-PU-237 HEDL       EVAL-APR78 MANN AND SCHENTER                 9431 1451    5
94-PU-238 HEDL,AI,+  EVAL-APR78 MANN,SCHENTER,ALTER,DUNFORD,+     9434 1451    5
94-Pu-239 LANL       EVAL-APR89 P.YOUNG, L.WESTON, W.POENITZ      9437 1451    5
94-PU-240 ORNL       EVAL-AUG86 L.W. WESTON AND E. D. ARTHUR      9440 1451    5
94-PU-241 ORNL       EVAL-OCT88 L.WESTON,R.WRIGHT,H,DERRIEN +     9443 1451    5
94-PU-242 HEDL,SRL,+ EVAL-OCT78 MANN,BENJAMIN,MADLAND,HOWERTON,+ 9446 1451    5
94-PU-243 BNL,SRL,+  EVAL-JUL76 KINSEY-ASSEMBLER(SEE COMMENTS)   9449 1451    5
94-PU-244 HEDL,SRL   EVAL-APR78 MANN,SCHENTER,BENJAMIN,MCCROSSON 9452 1451    5
95-AM-241 CNDC       EVAL-FEB88 ZHOU DELIN,GU FUHUA ET AL.        9543 1451    5
95-AM-242 SRL        EVAL-AUG75 BENJAMIN AND MCCROSSON            9546 1451    5
95-AM-242MHEDL,SRL,+ EVAL-APR78 MANN,BENJAMIN,HOWERTON,ET AL.     9547 1451    5
95-AM-243 ORNL,HEDL+ EVAL-OCT88 WESTON,MANN,HOWERTON,ET AL.       9549 1451    5
96-CM-241 HEDL       EVAL-APR78 MANN AND SCHENTER                 9628 1451    5
96-CM-242 HEDL,SRL,+ EVAL-APR78 MANN,BENJAMIN,HOWERTON,ET AL.     9631 1451    5
96-CM-243 HEDL,SRL,+ EVAL-APR78 MANN,BENJAMIN,HOWERTON,ET AL.     9634 1451    5
96-CM-244 HEDL,SRL,+ EVAL-APR78 MANN,BENJAMIN,HOWERTON,ET AL.     9637 1451    5
96-CM-245 SRL,LLNL   EVAL-JAN79 BENJAMIN AND HOWERTON             9640 1451    5
96-CM-246 BNL,SRL,+  EVAL-JUL76 KINSEY-ASSEMBLER(SEE COMMENTS)   9643 1451    5
96-CM-247 BNL,SRL,+  EVAL-JUL76 KINSEY-ASSEMBLER(SEE COMMENTS)   9646 1451    5
96-CM-248 HEDL,SRL,+ EVAL-APR78 MANN,BENJAMIN,HOWERTON,ET AL.     9649 1451    5
97-BK-249 CNDC       EVAL-JUN86 ZHOU DELIN ET. AL.                9752 1451    5
98-CF-249 CNDC       EVAL-APR89 ZHOU DELIN, SU ZHONGDI ET AL.     9852 1451    5
98-CF-250 BNL,SRL,+  EVAL-JUL76 KINSEY-ASSEMBLER(SEE COMMENTS)   9855 1451    5
98-CF-251 BNL,SRL,+  EVAL-JUL76 KINSEY-ASSEMBLER(SEE COMMENTS)   9858 1451    5
98-CF-252 BNL,SRL,+  EVAL-JUL76 KINSEY-ASSEMBLER(SEE COMMENTS)   9861 1451    5
98-CF-253 SRL        EVAL-DEC75 BENJAMIN AND MCCROSSON            9864 1451    5
99-ES-253 BNL,SRL    EVAL-JUL76 KINSEY,BENJAMIN, AND MCCROSSON    9913 1451    5
```

A.2 Index of the JEF-2.2 Nuclear Data File

```
90-TH-230 NEA        RCOM-JUN82 SCIENTIFIC CO-ORDINATION GROUP    9034 1451    5
90-TH-232 NEA        RCOM-JUN82 SCIENTIFIC CO-ORDINATION GROUP    9040 1451    5
91-PA-231 NEA        RCOM-JUN82 SCIENTIFIC CO-ORDINATION GROUP    9131 1451    5
91-PA-233 NEA        RCOM-JUN82 SCIENTIFIC CO-ORDINATION GROUP    9137 1451    5
```

```
92-U -232 NEA          RCOM-JUN82 SCIENTIFIC CO-ORDINATION GROUP    9219 1451    5
92-U -233 NEA          RCOM-JUN82 SCIENTIFIC CO-ORDINATION GROUP    9222 1451    5
92-U -234 NEA          RCOM-JUN82 SCIENTIFIC CO-ORDINATION GROUP    9225 1451    5
92-U -235 NEA          RCOM-AUG90 E. FORT, H.TELLIER                9228 1451    5
92-U -236 NEA          RCOM-JUN82 SCIENTIFIC CO-ORDINATION GROUP    9231 1451    5
92-U -237 NEA          RCOM-JUN82 SCIENTIFIC CO-ORDINATION GROUP    9234 1451    5
92-U -238 JEF COLLAB EVAL-JUN89 MCM,MGS,FHF,CN,YN,KANDA ET AL       9237 1451    5
```

A.3 Index of the JENDL-3 Nuclear Data File

```
88-RA-223 TIT          EVAL-AUG88 N.TAKAGI                          8825 1451    5
88-RA-224 TIT          EVAL-AUG88 N.TAKAGI                          8828 1451    5
88-RA-225 TIT          EVAL-AUG88 N.TAKAGI                          8831 1451    5
88-RA-226 TIT          EVAL-AUG88 N.TAKAGI                          8834 1451    5
89-AC-225 TIT          EVAL-AUG88 N.TAKAGI                          8925 1451    5
89-AC-226 TIT          EVAL-AUG88 N.TAKAGI                          8928 1451    5
89-AC-227 TIT          EVAL-AUG88 N.TAKAGI                          8931 1451    5
90-TH-227 TIT          EVAL-AUG88 N.TAKAGI                          9025 1451    5
90-TH-228 KINKI U.     EVAL-JUN87 T.OHSAWA                          9028 1451    5
90-TH-229 TIT          EVAL-AUG88 N.TAKAGI                          9031 1451    5
90-TH-230 KINKI U.     EVAL-JUL87 T.OHSAWA                          9034 1451    5
90-TH-232 KINKI U.     EVAL-MAR87 T.OHSAWA                          9040 1451    5
90-TH-233 KINKI U.     EVAL-JUL87 T.OHSAWA                          9043 1451    5
90-TH-234 KINKI U.     EVAL-JUL87 T.OHSAWA                          9046 1451    5
91-PA-231 KINKI U.+    EVAL-MAR87 T.OHSAWA, M.INOUE AND T.NAKAGAWA  9131 1451    5
91-PA-232 TIT          EVAL-AUG88 N.TAKAGI                          9134 1451    5
91-PA-233 KINKI U.+    EVAL-MAR87 T.OHSAWA, M.INOUE AND T.NAKAGAWA  9137 1451    5
92-U -232 KINKI U.+    EVAL-MAR87 T.OHSAWA AND T. NAKAGAWA          9219 1451    5
92-U -233 SAEI+        EVAL-MAR87 H.MATSUNOBU,Y.KIKUCHI,T.NAKAGAWA  9222 1451    5
92-U -234 KAWASAKI     EVAL-MAR87 T.WATANABE                        9225 1451    5
92-U -235 SAEI+        EVAL-MAR87 H.MATSUNOBU,K.HIDA,T.NAKAGAWA+    9228 1451    5
92-U -236 NAIG         EVAL-MAR88 T.YOSHIDA                         9231 1451    5
92-U -237 JAERI        EVAL-MAR93 T.NAKAGAWA                        9234 1451    5
92-U -238 KYU,JAERI+   EVAL-APR87 Y.KANDA ET AL.                    9237 1451    5
93-NP-236 JAERI        EVAL-MAR93 T.NAKAGAWA                        9343 1451    5
93-NP-237 KYUSHU U.+   EVAL-NOV87 Y.UENOHARA, Y.KANDA               9346 1451    5
93-NP-238 JAERI        EVAL-MAR93 T.NAKAGAWA                        9349 1451    5
93-NP-239 KYUSHU U.+   EVAL-MAR76 Y.KANDA, JENDL-CG                 9352 1451    5
```

Appendix B

NJOY Input Files

B.1 Input File for U^{238}

```
1/              interactive mode
6/              endfb 6 type nuclear data file
*moder*/        convert  from ASCII to binary
20 -21
*reconr*/       reconstruct resonance dependencies
-21 -22/        input - output tapes
*PENDF tape for u238 from endfb6 */ title for generated PENDF tape
9237 1/             MAT number
 0.05 0.  7 /
*92-u238 from endf6*/
0/              end of reconr module
*broadr*/       doppler broadening calculation
-22 -23/        input - output tapes
9237 3 0 1 0/   broadr options
0.05/           percent  error
300. 600. 900./ temperatures for doppler broadening
0/              end of broadr
*unresr*/       unresolved range calculation
-21 -23 -24/
9237 3 10 1 /
300. 600. 900./
1.E10 1.E4 3.6E3 1.E3 2.613E2 1.46E2 65.34 31.49 15.53 1.0 / sigma0 values
0/
*thermr*/       thermal scatterin  matrix calculation
0 -24 -26 /
0 9237 8 3 1 0 1 221 1 / the MT number for for scat matrix is 221 ( to be
300. 600. 900./          used in groupr and WIMSR )
0.01 4.0  /
*groupr*/       groupwise x-sec production
-21 -26 0 -25 /
9237 9 0 -5 1 3 10 1 / -5 means flux calculator
```

```
*92-u238 from endfb6 */
300. 600. 900./
1.E10 1.E4 3.6E3 1.E3 2.613E2 1.46E2 65.34 31.49 15.53 1.0 /
347.87 11.17 9000 -34  0 0 0 1 1.7E-7/ Flux Calculator options
3 /               generate multi-group x-sec for 300 K
3 221 /
3 252 /
3 452 /
3 455 /
6 /
6 221 /
0 /
3 /               generate multi-group x-sec for 600 K
3 221 /
3 252 /
3 452 /
3 455 /
6 /
6 221 /
0 /
3 /               generate multi-group x-sec for 900 K
3 221 /
3 252 /
3 452 /
3 455 /
6 /
6 221 /
0 /
0 /               end of groupr options
*wimsr*/          generate wims formatted multi-group file from
-25 27 /          groupr output
2 4 /
1 0 0 1/
9237 /
92 /
0 0 65.34   1 0.  221 0 1 1 0 0 / 65.34  is reference sigma0
.188 .188 .188 .188 .188 .188 .188 .188 .188 .188 .188 .188 .188/ Lambda
*stop*/  end of run for this material
```

B.2 Input File for U^{235}

```
1/ interactive mode
6/ input tape is endfb 6 formatted
*moder* /convert to bin
20 -21 /
*reconr*/
-21 -22/
*PENDF tape for u235 from endfb6 */
9228 1/
0.05 0. 7 /  error is 5 %
*92-u235 from endf6*/
0/
*broadr*/
-22 -23/
9228 3 0 1 0/ broadr run for 3 temperatures
0.05/
300. 600. 900./
0/
*unresr*/
-21 -23 -24/
9228 3  9  1/
300. 600.900./
1.E10 1.E4 3.6E3 1.E3 2.613E2 1.46E2 65.34 31.49 15.53 1.0 / sigma0
0/
*thermr*/
0 -24 -26 /
0 9228 8 3 1 0 1 221 1 /
300. 600. 900./
0.1 4.0/
*groupr*/
-21 -26 0 -25 /
9228 9 0 0  3 1 9  1 / fourth entry is IWT
*92-u235 from endfb6 (IWT=0)*/ IWT=0 means that flux calculator
300. 600. 900. / flux is to be used for weighting.
1.E10 1.E4 3.6E3 1.E3 2.613E2 1.46E2 65.34 31.49 15.53 1.0 /
-34/            ninwt tape unit e.g. tape34 is coming from u238...
3 / for 300 K
3 221/
3 251/
3 252/
3 253/
3 452/
3 455/
6 /
6 221 /
0/
3 / for 600 K
3 221/
3 251/
3 252/
3 253/
3 452/
3 455/
```

```
6 /
6 221 /
0/
3 / for 900 K
3 221/
3 251/
3 252/
3 253/
3 452/
3 455/
6 /
6 221 /
0/
0 /
*wimsr*/
-25 27 /
2 4 /
1 0 0 1/
9228/
92/
0 7  1.E10 1 0.  221 0 1 0  0 0 / reference sigma0 is 1.E10
.1965 .1965 .1965 .1965 .1965 .1965 .1965 .1965 .1965 .1965 .1965 .1965 .1965/
*stop*/
```

B.3 Input File for U^{233}

```
1/ batch mode
6/ endfb 6
*moder* /convert to binary
20 -21 /
*reconr*/ reconstruct reso data
-21 -22/
*PENDF tape for u233 from endfb6 */
9222 1/
0.05 0. 7 /
*92-u235 from endf6*/
0/
*broadr*/
-22 -23/
9222 3 0 1 0/
0.05/ error is 5 %
300. 600. 900./
```

```
0/
*unresr*/
-21 -23 -24/
9222 3  10  1/
300. 600. 900./
1.E10 1.E4 3.6E3 1.E3 8E2  4E2 100  31.49 15.53 1.0 / sigma0 values.
0/
*thermr*/
0 -24 -26 /
0 9222 8 3 1 0 1 221 1 /
300. 600. 900/
0.05 4.0/
*groupr*/  produce multigroup data
-21 -26 0 -25 /
9222 9 0 -5 1 3 10  1 /   EPRI-CPM flux for weighting
*92-u233 from endfb6 (IWT=-5)*/
300. 600. 900. /
1.E10 1.E4 3.6E3 1.E3 8E2 4E2 100  31.49 15.53 1.0 /
1.E3 11.17 6000/
3 / for 300 K
3 221/
3 251/
3 252/
3 253/
3 452/
3 455/
6 /
6 221 /
0/
3 / for 600 K
3 221/
3 251/
3 252/
3 253/
3 452/
3 455/
6 /
6 221 /
0/
3 / for 900 K
3 221/
3 251/
3 252/
3 253/
3 452/
3 455/
6 /
6 221 /
0/
0
*wimsr*/
-25 27 /
2 4 /
1 0 0 1/
9222/
```

```
92/
0 7  1.E10 1 0.  221 0 1 0  0 0 / reference sigma0 is 1.E10
.2 .2 .2 .2 .2 .2 .2 .2 .2 .2 .2 .2 / lambda is 0.2
*stop*/
```

B.4 Input File for Th^{232}

```
1/ interactive mode
6/ endfb 6
*moder*/
20 -21/
*reconr*/ reconstruct resonances
-21 -22
*PENDF tape for TH-232 from endfb6 */
9040  1/
 0.05 0.  7 /
*92-th232  from endf6*/
0/
*broadr*/ doppler broadening
-22 -23/
9040  3 0 1 0/
0.05/
300. 600. 900./
0/
*unresr*/ unresolved range
-21 -23 -24/
9040 3 10 1 /
300. 600. 900./
1.E10 1.E4 3.E3 1.E3 8.E2 4.E2 1.E2 5.E1 1.E1 1./ sigma0 values
0/
*thermr*/ thermal scat matrix
0 -24 -26 /
0 9040  8 3 1 0 1 221 1 /
300. 600. 900./
0.01 4.0  /
*groupr*/ groupwise x-sec prod.
-21 -26 0 -25 /
9040  9 0 -5 1 3 10 1 / IWT=-5 means flux calculation case.
*90-TH232  from endfb6 */
300. 600. 900./
1.E10 1.E4 3.E3 1.E3 8.E2 4.E2 1.E2 5.E1 1.E1 1./
347.87 11.17 9000 -34  0 0 0 1 1.7E-7/ FOR TH232 + H homogen mix /
```

```
3 / for 300 K
3 221 /
3 252 /
3 452 /
3 455 /
6 /
6 221 /
0 /
3 / for 600 K
3 221 /
3 252 /
3 452 /
3 455 /
6 /
6 221 /
0 /
3 / for 900 K
3 221 /
3 252 /
3 452 /
3 455 /
6 /
6 221 /
0 /
0 /
*wimsr*/
-25 27 /
2 4 /
1 0 0 1/
9040 /
90/
0 0 50.0  1 0.  221 0 1 1 0 0 / reference sigma0 is 50 barn .
.1965 .1965 .1965 .1965 .1965 .1965 .1965 .1965 .1965 .1965 .1965 .1965/
*stop*/
```

B.5 Input File for Aluminum

```
0/
6/
*moder*/
20 -21 /
*reconr*/
-21 -22/
*pendf tape for al27*/
1325  1 /
0.05 / fractional error is 5 %
*AL-27*/
0/
*broadr* / broaden to 300K
-22 -23 /
```

```
1325  1 0 1 0 /
0.005 /
300./
0/
*unresr*/
-21 -23 -24 /
1325  1 9  1/
300./
1.E10 1.E4 3.6E6 1.E3 2,613E2 1.462E2 65.34 31.49 15.53  /
0/
*thermr*
0  -24 -26/
0   1325  8 1 1  0 1  221 1
300./
0.01 4.0/
*groupr*/
-21 -26 0 -25 /
1325  9 0 5 1 1 9  1 / EPRI-CPM flux
*13-al27 from enfb6*/
300./
1.E10 1.E4 3.6E6 1.E3 2,613E2 1.462E2 65.34 31.49 15.53  /
3 /
3 221 /
3 252 /
6 /
6 221 /
0 /
0 /
*wimsr*/
-25 27 /
2 4 /
1 0 0 1/
1325  /
13 /
1 0 1.E10  0 0. 221 0 0 1 0 0 /
1. 1. 1. 1. 1. 1. 1. 1. 1. 1. 1. 1. 1. /
*stop*
```

B.6 Input File for Oxygen

```
0/
6/
*moder*/
20 -21 /
*reconr*/
-21 -22/
*pendf tape for o16*/
825 1 /
0.02 / 0. 7 0.002 / 0.001/
*8-o-16 from endfb6 */
```

```
0/
*broadr* /
-22 -24 /
825 1 0 1 0 /
0.05 / fractional error is 5 %
300./
0/
*thermr*
0  -24 -26/
0  825 8 1 1 0 1  221 1/
300./
0.01 4.0/
*groupr*/
-21 -26 0 -25 /
825 9 0 -5 1 1 1  1 /
*16-o-8 from enfb6*/
300./
1.E10/
347.87 11.17 9000/
3 / for 300 K
3 221/
3 252/
0 /
0 /
*wimsr*/
-25 27 /
2 4 /
1 0 0 1/
825 /
8
1 0 1.E10  0 0. 221 0 0 1 0 0 /
1. 1. 1. 1. 1. 1. 1. 1. 1. 1. 1. 1. 1. /
*stop*
```

B.7 Input File for Hydrogen Bound in Water

```
0/
6/
*moder*/
20 -21 /
*moder*/
30 -31 / convert thermal scattering data to binary
*reconr*/
-21 -22/
*pendf tape for h1*/
125 1 /
0.002 / 0. 7 0.002 / 0.001/
*1-H1(H2O)*/
0/
*broadr* /
```

```
-22 -23 /
125 1 0 1 0 /
0.05 /
300./
0/
*unresr*/
-21 -23 -24 /
125 1 5 1/
300./
1.E10 1.E4 1.E3 1.E2 1.E1 / 5 sigma0 values
0/
*thermr*
-31 -24 -26/  compute thermal scattering matrix using data in tape31
1  125 8 1 4 0 2 221 1 /
300./
0.01 4.0/
*groupr*/
-21 -26 0 -25 /
125 9 0 5 1 1 5 1 /
*1-h-1 from enfb6*/
300./
1.E10 1.E4 1.E3 1.E2 1.E1 /
3 /
3 221 /
3 252 /
6 /
6 221 /
0 /
0 /
*wimsr*/
-25 27 /
2 4 /
1 0 0 1/
125 /
1
1 0 1.E10 0 0. 221 0 0 1 0 0 /
1. 1. 1. 1. 1. 1. 1. 1. 1. 1. 1. 1. 1. /
*stop*
```

Appendix C

WIMS Inputs for Benchmark Assemblies

C.1 TRX Input

The Input Listing Below belowngs to TRX-1. The same input, but with different pitch and buckling values is valid for TRX-2.

```
*WIMS INPUT FOR TRX-1  ( ENDFB-VI version_)
**************************************************
CELL      6
SEQUENCE  1
NGROUP    18 2
NMESH     10
NREGION   4  0   4
NMATERIAL 3
NREACT    2
PREOUT
INITIATE
ANNULUS 1 0.4915 1
ANNULUS 2 0.5042 0
ANNULUS 3 0.5753 2
ANNULUS 4 0.94822 3
FEWGROUP 2 3 4 5 6 7 9 12 16 20 23 27 45 54 57 60 63 69
MESH 4 1 1 4
MATERIAL 1 -1 293.0 1 9228.1 .0006253 9237.1  .047205
MATERIAL 2 -1 293.0 2  1325  0.06025
MATERIAL 3 -1 293.0 3 125  .06676  825  .03338
REGULAR 1 6
S 4
```

```
BEGINC
THERMAL 6
BEEONE 1
DNB  1 0. 0. 0. 0.
DNB  2 0. 0. 0. 0.
DNB  3 0.06676  0. 0.03338 0.
BUCKLINGS 0.005174 0.000526
DIFFUSION 1 3 1
LEAKAGE   5
REACTION (9228,293.0) (9237,293.0)
PARTITION 45 69
BEGINC
************************************************************
```

C.2 BAPL Input

Below is the input for BAPL-1. Substituting the necessary pitch and buckling values make this input also valid for BAPL-2 and BAPL-3.

```
*WIMS INPUT FOR BAPL-1,  ENDF/B-VI version
************************************************************
CELL      6
SEQUENCE  1
NGROUP   18 2
NMESH    10
NREGION   4  0   4
NMATERIAL 3
NREACT    2
PREOUT
INITIATE
ANNULUS 1 0.4864 1
ANNULUS 2 0.5042 0
ANNULUS 3 0.5753 2
ANNULUS 4 0.81790  3
FEWGROUP 2 3 4 5 6 7 9 12 16 20 23 27 45 54 57 60 63 69
MESH 4 1 1 4
MATERIAL 1 -1 293.0 1 9228.1  0.0003112  9237.1 .023127 825  .046946
MATERIAL 2 -1 293.0 2  1325  0.06025
MATERIAL 3 -1 293.0 3 125  .06676  825  .03338
REGULAR 1 6
S 4
BEGINC
THERMAL 6
BEEONE 1
DNB  1 0. 0. 0. 0.
DNB  2 0. 0. 0. 0.
DNB  3 0.06676  0. 0.03338 0.
BUCKLINGS 0.002734 0.000525
```

```
DIFFUSION 1 3 1
LEAKAGE   5
REACTION (9228,293.0) (9237,293.0)
PARTITION 45 69
BEGINC
*********************************************************************
```

C.3 BNL Input

Like for TRX and BAPL the input below is for BNL-1. The input also holds for BNL-2 and BNL-3 if the correct pitch and bucling values are substituted.

```
* WIMS INPUT FOR BNL-1
*************************************************************************
CELL 6
SEQUENCE 1
NGROUP 69,2
NMESH 32
NREGIONS  3,0,3
NMATERIALS  3,0
NREACT 2
PREOUT
INITIATE
MATERIAL 1, -1,293,1, 16, 4.08832E-2, 9040.1 , 1.98115E-2, 9222.1, $
 6.1021E-4
MATERIAL 2, -1, 293,2, 91, 4.4355E-2
MATERIAL 3, -1, 293,3, 2001, 6.676E-2, 16, 3.338E-2
ANNULUS 1, .546100,1
ANNULUS 2, .633730,2
ANNULUS 3, .836017,3
REGULAR 1 6
 FEWGROUPS  1 2 3 4 5 6 7 8 9 10 11 12 13 14 15 16 17 18 19 $
20 21 22 23 24 25 26 27 28 29 30 31 32 33 34 35 36 37 38 $
39 40 41 42 43 44 45 46 47 48 49 50 51 52 53 54 55 56 $
57 58 59 60 61 62 63 64 65 66 67 68 69
MESH 12 8 12
S 12
BEGINC
THERMAL 24
PARTITION 45 69
BUCKLING 1.0E-10,75.88E-4
NOBUCKLING
REACTION 9040.1, 293, 9222.1,293
BEGINC
*************************************************************************]
```

Appendix D

Listing of Utility Programs

D.1 Program Libdiv

The Libdiv program splits the original WIMS library into many files each containing a single material. Each file is complete and consistent. There is no data loss during the splitting process.

```
      PROGRAM LIBDIV
CMS    THIS PROGRAM SPLIT THE MASTER LIB OF WIMS INTO INDIVIDUAL FILES
      DIMENSION WS(2000,200),IWS(2000,200), WSA(2000),WSB(2000),WSE
     +(2000)
      INTEGER LZ,NZ,N0Z,N1Z,N2Z,N3Z,NNF,NNFP,IN(200),ID(200)
      REAL*4 GB(200),FIS(100)
      INTEGER JC(200),JB(200),JA
      REAL*4 AA(200,200)
      INTEGER IM(200),NF(200),NT(200),NZZ(200),IAN(200)
      REAL*4 AW(200)
      REAL*4 PSCAT(100,200), XISS(100,200), TR(200,200), ABS(200,200),
     +CHI(100,200),ALAMDA(100,200)
      REAL*4 XNUFIS(200,200),FIS4(200,200)
      INTEGER KK(200),KK6(200,10),IDUF(200)
      REAL*4 AA4(5000,200)
      REAL*4 TEMP(10,200)
      REAL*4 TR6(200,10,200),ABS6(200,10,200),XNUFIS6(200,10,200),FIS6
     +(200,10,200), AA6(5000,10,200)
      INTEGER*4 M1(50,100),M2(50,100),MM1,MM2,M3(20,100)
      REAL*4 TRES(200,50,100),SIGPR(200,50,100),RSIGR(200,10,50,100)
      REAL*4 XIDN(50,100)
      REAL*4 P1SCAT(300,300,4)
      CHARACTER*5 DUMF
      CHARACTER*4 ALDO
```

```
      INTEGER I,J,IARGC
      EQUIVALENCE (WS(1,1),IWS(1,1))
      DATA A/'ALDO'/
      PRINT*,' NOW IN PROGRAM'
      OPEN(1,FILE='MASTER.LIB',FORM='FORMATTED')
      REWIND 1
      IEND=999999999
      FEND=9.99999999E+8
      IK1=0
      READ(1,440) LZ,NZ,N0Z,N1Z,N2Z,N3Z,NNF,NNFP
      PRINT 440, LZ,NZ,N0Z,N1Z,N2Z,N3Z,NNF,NNFP
      NNLSZ=N1Z+1
      NN2Z=N1Z+N2Z
      NN4Z=NN2Z+1
      READ(1,440) (ID(J),J=1,LZ)
      READ(1,450) (GB(J),J=1,NZ+1)
      READ(1,450) (FIS(J),J=1,N0Z)
      DO 100 J=1,1000
         READ(1,440) JC(J)
         IF(JC(J)-IEND)10,110,10
   10    JCC=JC(J)/6
         IF(JCC)50,50,20
   20    JJ=1
   30    JJJ=JJ+5
         READ(1,490) WS(JJ,J),IWS(JJ+1,J),WS(JJ+2,J),IWS(JJ+3,J),WS
     +   (JJ+4,J),IWS(JJJ,J)
         JCC=JCC-1
         IF(JCC)50,50,40
   40    JJ=JJ+6
         GO TO 30
   50    JCC=JC(J)-6*(JC(J)/6)
         IF(JCC)90,90,60
   60    GO TO (50,70,50,80),JCC
   70    JJ=JC(J)-1
         READ(1,490) WS(JJ,J),IWS(JJ+1,J)
         GO TO 90
   80    JJ=JC(J)-3
         READ(1,490) WS(JJ,J),IWS(JJ+1,J),WS(JJ+2,J),IWS(JJ+3,J)
   90    CONTINUE
         IDUF(J)=IWS(JC(J),J)
  100 CONTINUE
  110 WRITE(2) A
      DO 170 J=1,LZ
         READ(1,460) IM(J),AW(J),IAN(J),NF(J),NT(J),NZZ(J)
         IK1=IK1+NZZ(J)
         READ(1,450) (PSCAT(JA,J),JA=1,N2Z),(XISS(JA,J),JA=1,N2Z),(TR
     +   (JA,J),JA=1,N2Z+N1Z),(ABS(JA,J),JA=1,N1Z+N2Z),(CHI(JA,J),JA=1,
     +   N2Z),(ALAMDA(JA,J),JA=1,N2Z)
         IF(NF(J)-2)130,120,120
  120    READ(1,450) (XNUFIS(JA,J),JA=1,N1Z+N2Z),(FIS4(JA,J),JA=1,N1Z
     +   +N2Z)
  130    READ(1,440) KK(J)
         READ(1,450) (AA4(JA,J),JA=1,KK(J))
         DO 160 I=1,NT(J)
            READ(1,450) (TR6(JA,I,J),JA=N1Z+N2Z+1,NZ),(ABS6(JA,I,J),JA
```

```
     +      =N1Z+N2Z+1,NZ)
            IF(NF(J)-2)150,140,140
140         READ(1,450) (XNUFIS6(JA,I,J),JA=N1Z+N2Z+1,NZ),(FIS6(JA,I,J),
     +      JA=N1Z+N2Z+1,NZ)
150         READ(1,440) KK6(J,I)
            READ(1,450) (AA6(JA,I,J),JA=1,KK6(J,I))
160      CONTINUE
         READ(1,440)JA
170   CONTINUE
      DO 180 I=NNLSZ,NN2Z
         DO IJ=1,IK1
            READ(1,440,ERR=430) M3(I,IJ)
            READ(1,470) XIDN(I,IJ),M1(I,IJ),M2(I,IJ)
            MM1=M1(I,IJ)
            MM2=M2(I,IJ)
            READ(1,450) (TRES(JD,I,IJ),JD=1,MM1),(SIGPR(JD,I,IJ),JD=1,
     +      MM2),((RSIGR(JA,JZ,I,IJ),JA=1,MM2),JZ=1,MM1)
         END DO
         READ(1,440) IDUM
         READ(1,470) ZDUM
         READ(1,450) ZDUM
         READ(1,440) IDUM
180   CONTINUE
      PRINT*,' NOW P1 SCATTER'
      DO 200 K=1,4
         DO 190 I=1,NZ
            READ(1,450) (P1SCAT(JA,I,K),JA=1,NZ)
190      CONTINUE
200   CONTINUE
      LZDUM=1
      IRES=1
      DO 420 J=1,LZ
         IDUM1=0
         IDUM2=0
         DUMF='    '
         WRITE(DUMF,'(I5)') ID(J)
         OPEN(12,FILE=DUMF,STATUS='NEW')
         IF(NF(J).GT.1) IDUM1=1
         IF(IDUF(J).EQ.-1) IDUM2=1
         WRITE(12,440) LZDUM,NZ,N0Z,N1Z,N2Z,N3Z,IDUM1,IDUM2
         WRITE(12,440) ID(J)
         WRITE(12,450) (GB(I),I=1,NZ+1)
         WRITE(12,450) (FIS(I),I=1,N0Z)
         WRITE(12,440) JC(J)
         IF(JC(J)-IEND)210,300,210
210      JCC=JC(J)/6
         IF(JCC)250,250,220
220      JJ=1
230      JJJ=JJ+5
         WRITE(12,490) WS(JJ,J),IWS(JJ+1,J),WS(JJ+2,J),IWS(JJ+3,J),WS
     +   (JJ+4,J),IWS(JJJ,J)
         JCC=JCC-1
         IF(JCC)250,250,240
240      JJ=JJ+6
         GO TO 230
```

```
250     JCC=JC(J)-6*(JC(J)/6)
        IF(JCC)290,290,260
260     GO TO (250,270,250,280),JCC
270     JJ=JC(J)-1
        WRITE(12,490) WS(JJ,J),IWS(JJ+1,J)
        GO TO 290
280     JJ=JC(J)-3
        WRITE(12,490) WS(JJ,J),IWS(JJ+1,J),WS(JJ+2,J),IWS(JJ+3,J)
290     CONTINUE
300     CONTINUE
        WRITE(12,440) IEND
        WRITE(12,460) IM(J),AW(J),IAN(J),NF(J),NT(J),NZZ(J)
        WRITE(12,450) (PSCAT(JA,J),JA=1,N2Z),(XISS(JA,J),JA=1,N2Z),(TR
   +    (JA,J),JA=1,N2Z+N1Z),(ABS(JA,J),JA=1,N1Z+N2Z),(CHI(JA,J),JA=1,
   +    N2Z),(ALAMDA(JA,J),JA=1,N2Z)
        IF(NF(J)-2)320,310,310
310     WRITE(12,450) (XNUFIS(JA,J),JA=1,N1Z+N2Z),(FIS4(JA,J),JA=1,N1Z
   +    +N2Z)
320     WRITE(12,440) KK(J)
        WRITE(12,450) (AA4(JA,J),JA=1,KK(J))
        WRITE(12,450) (TEMP(JT,J),JT=1,NT(J))
        DO 350 I=1,NT(J)
           WRITE(12,450) (TR6(JA,I,J),JA=N1Z+N2Z+1,NZ),(ABS6(JA,I,J),
   +       JA =N1Z+N2Z+1,NZ)
           IF(NF(J)-2)340,330,330
330        WRITE(12,450) (XNUFIS6(JA,I,J),JA=N1Z+N2Z+1,NZ),(FIS6
   +       (JA,I,J),JA=N1Z+N2Z+1,NZ)
340        WRITE(12,440) KK6(J,I)
           WRITE(12,450) (AA6(JA,I,J),JA=1,KK6(J,I))
350     CONTINUE
        WRITE(12,440) IEND
        IRC=0
        IF(NF(J).EQ.0.OR.NF(J).EQ.4) GO TO 400
        IF(NF(J).EQ.1.OR.NF(J).EQ.2) THEN
           IRC=1
           GOTO 360
        END IF
        IF(NF(J).EQ.3) IRC=2
360     IRD=IRES
        IZK=IZK+NZZ(J)
        DO 390 IR=NNLSZ,NN2Z
370        DO IIR=1,NZZ(J)
              IZ=IZK+IIR-NZZ(J)
380           WRITE(12,440) M1(IR,IZ)*M2(IR,IZ)
              WRITE(12,470) XIDN(IR,IZ),M1(IR,IZ),M2(IR,IZ)
              MM1=M1(IR,IZ)
              MM2=M2(IR,IZ)
              WRITE(12,450) (TRES(JD,IR,IZ),JD=1,MM1),(SIGPR(JD,IR,IZ),
   +          JD=1,MM2),((RSIGR(JA,JZ,IR,IZ),JA=1,MM2),JZ=1,MM1)
           END DO
           WRITE(12,480) 0.0,1,1,0.0,0.0,0.0
           WRITE(12,440)IEND
           IRES=IRD
390     CONTINUE
400     IF(J.LE.4) THEN
```

```
            DO 410 I=1,NZ
               WRITE(12,450) (P1SCAT(JA,I,J),JA=1,NZ)
  410       CONTINUE
          END IF
          IF(NF(J).NE.0.AND.NF(J).LT.4)PRINT*,' RESO NUC IS ',ID(J),XIDN
     +    (NNLSZ,IRES),' JA AND IRES=',J,IRES
          IRES=IRES+IRC*IKAK
          CLOSE(12)
  420 CONTINUE
      STOP
  430 PRINT*,'ERROR IN RESO READ ?' ,M,I,J
      STOP
  440 FORMAT(5I15)
  450 FORMAT(5E15.8)
  460 FORMAT(I6,E15.8,4I6)
  470 FORMAT(E15.8,2I6)
  480 FORMAT(E11.4,2I6,4E11.4)
  490 FORMAT(E15.8,I6,E15.8,I6,E15.8,I6)
  500 FORMAT(6(I6,E15.8))
      END
```

D.2 Program Libgen

The Libgen program produces a Binary WIMS library from the individual files. The user can select the number of elements to be included in the produced library. The non-standard structure of WIMSR generated multigroup files is taken into account and processed appropriately.

```
      PROGRAM LIBGEN
CMS    THIS PROGRAM COMBINES THE SPLITTED  MASTER LIB OF WIMS
CMS    WITH ENDF GENERATED DATA.
      DIMENSION WS(2000,200),IWS(2000,200)
      INTEGER LZ,NZ,N0Z,N1Z,N2Z,N3Z,NNF,NNFP,IN(200),ID(200)
      INTEGER IDD(200)
      REAL*4 GB(200),FIS(150)
      INTEGER JC(200),JB(200),JA
      REAL*4 AA(200,200)
      INTEGER IM(200),NF(200),NT(200),NZZ(200),IAN(200),INDAT(10)
      REAL*4 AW(200)
      REAL*4 PSCAT(150,200), XISS(150,200), TR(200,200), ABS(200,200),
     +CHI(150,200),ALAMDA(150,200)
      REAL*4 XNUFIS(200,200),FIS4(200,200)
      INTEGER KK(200),KK6(200,10),IDUF(200)
      REAL*4 AA4(5000,150)
      REAL*4 TEMP(10,150)
      REAL*4 TR6(150,10,200),ABS6(150,10,200),XNUFIS6(150,10,200),FIS6
```

```
     +(150,10,200), AA6(5000,10,200)
      INTEGER*4 M1(150,150),M2(150,150),MM1,MM2,M3(150,150)
      REAL*4 TRES(150,50,150),SIGPR(150,50,150), RSIGR(150,10,50,150)
      REAL*4 XIDN(150,150), FSPECT(200),P1WSRS(5000),P1SCAT(300,300,10)
      CHARACTER*5 DUMF
      INTEGER*4 ALDO
      INTEGER I,J,IARGC
      EQUIVALENCE (WS(1,1),IWS(1,1))
      DATA A/4HALDO/
      PRINT*,' NOW IN PROGRAM'
      OPEN(10,FILE='ZBIN.INP')
      OPEN(2,FILE='MASTER.BIN',FORM='UNFORMATTED')
      IEND=999999999
      FEND=9.99999999E+8
      READ(10,'(I5)') IFIL
      LZ=0
      IRZ=0
      IRZE=0
      NNFP=0
      NNF=0
      IKAK=0
      IP1=0
      IPP1=0
      DO 10 J=1,IFIL
         READ(10,'(I5)') IDD(J)
   10 CONTINUE
      DO 280 J=1,IFIL
         WRITE(DUMF,'(I5)') IDD(J)
         OPEN(12,FILE=DUMF,STATUS='OLD')
         IF(IDD(J).GE.10000) GO TO 120
         READ(12,410) LZDUM,NZ,N0Z,N1Z,N2Z,N3Z,IDUM1,IDUM2
         NNLSZ=N1Z+1
         NN2Z=N1Z+N2Z
         NN4Z=NN2Z+1
         IF(IDUM2.GT.0) NNFP=NNFP+1
         IF(IDUM1.GT.0) NNF=NNF+1
         READ(12,410) ID(J)
         READ(12,420) (GB(I),I=1,NZ+1)
         READ(12,420) (FIS(I),I=1,N0Z)
         READ(12,410) JC(J)
         IF(JC(J)-IEND)20,110,20
   20    JCC=JC(J)/6
         IF(JCC)60,60,30
   30    JJ=1
   40    JJJ=JJ+5
         READ(12,460) WS(JJ,J),IWS(JJ+1,J),WS(JJ+2,J),IWS(JJ+3,J),WS
     +   (JJ+4,J),IWS(JJJ,J)
         JCC=JCC-1
         IF(JCC)60,60,50
   50    JJ=JJ+6
         GO TO 40
   60    JCC=JC(J)-6*(JC(J)/6)
         IF(JCC)100,100,70
   70    GO TO (60,80,60,90),JCC
   80    JJ=JC(J)-1
```

```
      READ(12,460) WS(JJ,J),IWS(JJ+1,J)
      GO TO 100
 90   JJ=JC(J)-3
      READ(12,460) WS(JJ,J),IWS(JJ+1,J),WS(JJ+2,J),IWS(JJ+3,J)
100   CONTINUE
110   CONTINUE
      READ(12,410) IEND
120   LZ=LZ+1
      IFIS1=0
      READ(12,430) IM(J),AW(J),IAN(J),NF(J),NT(J),NZZ(J),IFIS1
      ID(J)=IM(J)
      READ(12,420) (PSCAT(JA,J),JA=1,N2Z),(XISS(JA,J),JA=1,N2Z),(TR
     +(JA,J),JA=1,N2Z+N1Z),(ABS(JA,J),JA=1,N1Z+N2Z),(CHI(JA,J),JA=1,
     +N2Z),(ALAMDA(JA,J),JA=1,N2Z)
      IF(NF(J)-2)140,130,130
130   READ(12,420) (XNUFIS(JA,J),JA=1,N1Z+N2Z),(FIS4(JA,J),JA=1,N1Z
     ++N2Z)
140   READ(12,410) KK(J)
      READ(12,420) (AA4(JA,J),JA=1,KK(J))
      READ(12,420) (TEMP(JT,J),JT=1,NT(J))
      DO 170 I=1,NT(J)
         READ(12,420) (TR6(JA,I,J),JA=N1Z+N2Z+1,NZ),(ABS6(JA,I,J),JA
     +      =N1Z+N2Z+1,NZ)
         IF(NF(J)-2)160,150,150
150      READ(12,420) (XNUFIS6(JA,I,J),JA=N1Z+N2Z+1,NZ),(FIS6
     +   (JA,I,J),JA=N1Z+N2Z+1,NZ)
160      READ(12,410) KK6(J,I)
         READ(12,420) (AA6(JA,I,J),JA=1,KK6(J,I))
170   CONTINUE
      READ(12,410,ERR=400) IEND
      IRC=0
      IF(NF(J).EQ.0.OR.NF(J).EQ.4) GO TO 230
      IF(NF(J).EQ.1.OR.NF(J).EQ.2) THEN
         IRC=1
         GOTO 180
      END IF
      IF(NF(J).EQ.3.AND.NZZ(J).EQ.1) NZZ(J)=2
180   CONTINUE
      DO 220 IR=NNLSZ,NN2Z
         IRZ=IRZE
190      DO 210 IIR=1,NZZ(J)
            IRZ=IRZ+1
200         READ(12,410) M3(IR,IRZ)
            READ(12,440) XIDN(IR,IRZ),M1(IR,IRZ),M2(IR,IRZ)
            MM1=M1(IR,IRZ)
            MM2=M2(IR,IRZ)
            READ(12,420) (TRES(JD,IR,IRZ),JD=1,MM1),(SIGPR
     +      (JD,IR,IRZ),JD=1,MM2),((RSIGR(JA,JZ,IR,IRZ),JA=1,MM2),JZ
     +      =1,MM1)
210      CONTINUE
         IF(IR.EQ.NN2Z) IRZE=IRZ
         IF(IDD(J).LT.10000) READ(12,450) ZDUM
         READ(12,450) IDUM
220   CONTINUE
230   CONTINUE
```

```
      IF(IFIS1.EQ.1) READ(12,420) (FSPECT(IJ),IJ=1,NOZ)
      IF(IDD(J).GT.20000) GO TO 240
      IF(IDD(J).EQ.2001.OR.IDD(J).EQ.4001.OR.IDD(J).EQ.9001.OR.IDD(J)
     +  .EQ.4002) GO TO 250
      GO TO 280
240   IPP1=IPP1+1
      READ(12,410) INDAT(IPP1)
      READ(12,'(1PE15.8)') (P1WSRS(IK),IK=1,INDAT(IPP1))
      PRINT*,'INDAT=',INDAT(IPP1)
      GOTO 270
250   IP1=IP1+1
      DO 260 IZ=1,NZ
         READ(12,420) (P1SCAT(JA,IZ,IP1),JA=1,NZ)
260   CONTINUE
270   CLOSE(12)
280 CONTINUE
    WRITE(2) LZ,NZ,NOZ,N1Z,N2Z,N3Z,NNF,NNFP
    WRITE(2) (ID(J),J=1,IFIL)
    WRITE(2) (GB(I),I=1,NZ+1)
    WRITE(2) (FIS(I),I=1,NOZ)
    DO 290 J=1,IFIL
       IF(IDD(J).GE.10000) GO TO 290
       WRITE(2) JC(J),(WS(JA,J),JA=2,JC(J))
290 CONTINUE
300 WRITE(2) A
    DO 360 J=1,IFIL
       WRITE(2) IM(J),AW(J),IAN(J),NF(J),NT(J),NZZ(J)
       WRITE(2) (PSCAT(JA,J),JA=1,N2Z),(XISS(JA,J),JA=1,N2Z),(TR
     +  (JA,J),JA=1,N2Z+N1Z),(ABS(JA,J),JA=1,N1Z+N2Z),(CHI(JA,J),JA=1,
     +  N2Z),(ALAMDA(JA,J),JA=1,N2Z)
       IF(NF(J)-2)320,310,310
310    WRITE(2) (XNUFIS(JA,J),JA=1,N1Z+N2Z),(FIS4(JA,J),JA=1,N1Z+N2Z)
320    WRITE(2) KK(J) ,(AA4(JA,J),JA=1,KK(J))
       WRITE(2) (TEMP(JT,J),JT=1,NT(J))
       DO 350 I=1,NT(J)
          WRITE(2) (TR6(JA,I,J),JA=N1Z+N2Z+1,NZ),(ABS6(JA,I,J),JA=N1Z
     +    +N2Z+1,NZ)
          IF(NF(J)-2)340,330,330
330       WRITE(2) (XNUFIS6(JA,I,J),JA=N1Z+N2Z+1,NZ),(FIS6(JA,I,J),JA
     +    =N1Z+N2Z+1,NZ)
340       WRITE(2) KK6(J,I),(AA6(JA,I,J),JA=1,KK6(J,I))
350    CONTINUE
       WRITE(2) A
360 CONTINUE
    DO 370 I=NNLSZ,NN2Z
       DO J=1,IRZE
          IREZ=0
          MM1=M1(I,J)
          MM2=M2(I,J)
          WRITE(2) XIDN(I,J),M1(I,J),M2(I,J),(TRES(JD,I,J),JD=1,MM1),
     +    (SIGPR(JD,I,J),JD=1,MM2),((RSIGR(JA,JZ,I,J),JA=1,MM2),JZ=1,
     +    MM1)
       END DO
       WRITE(2) 0.0,1,1,0.0,0.0,0.0
       WRITE(2) A
```

```
370 CONTINUE
    DO 390 IK=1,IP1
       DO 380 IZ=1,NZ
          WRITE(2) (P1SCAT(JA,IZ,IK),JA=1,NZ)
380    CONTINUE
390 CONTINUE
    IF(IPP1.GT.0) THEN
       DO I=1,IPP1
          WRITE(2)(P1WSRS(II),II=1,INDAT(IPP1))
       END DO
    END IF
    WRITE(2) A
    ENDFILE 2
    REWIND 2
    STOP
400 PRINT*,' READ ERROR IN LINE 137'
410 FORMAT(5I15)
420 FORMAT(5E15.8)
430 FORMAT(I6,E15.8,5I6)
440 FORMAT(E15.8,2I6)
450 FORMAT(E11.4,2I6,4E11.4)
460 FORMAT(E15.8,I6,E15.8,I6,E15.8,I6)
470 FORMAT(6(I6,E15.8))
    END
```

ÇOK-ORTAMLI BİR BİLGİ YÖNETİM SİSTEMİ

Mehmet Erol Şanlıtürk

Veri tabanı teknolojisi, 1970 ve 1995 yılları arasında topluma çok önemli katkılarda bulundu ve sıra-düzensel, ağ, ve özellikle ilişkisel veri tabanı türleri olarak önemsenecek düzeyde gelişti. Donamımdaki gelişmelerle, veri tabanı alanında da nesneye-yönelik, uzman, çok-ortamlı veri tabanları ve bilgi sistemleri olarak yeni düşünceler oluştu.

Sunulacak olan sistem en az üç ana parçası olan nesneye-yönelik bir veri tabanı yönetim sistemidir: Uygulama veri tabanı, uygulama veri tabanının tanım veri tabanı, ve kullanıcıların uygulama veri tabanı üzerindeki yetkilerinin yönetimi için bir kullanıcılar veri tabanı. Zorunlu olmamakla birlikte, eğer uygulama veri tabanı için kurallar konulacaksa, uygulama veri tabanı üzerindeki mantıksal sonuç çıkarmalar için kullanılacak bir kural veri tabanı tanımlamak gereklidir. Sistemin diğer önemli bir yönü, veri tabanı tanımının, kullanıcılar veri tabanının ve kural tabanının da sistem tarafından yönetilen veri tabanları olmalarıdır.

Veri tabanlarının elemanları, cebirsel hesaplamalarla mantıksal sonuç çıkarma yeteneği olan nesneleri içeren sınıflardır. Nesnelerin çok-ortamlı elemanları, ve bir veri tabanında bir çok sınıflar olabilir. Her bir nesne, bir ana form ve, gerekli olursa, ana form ile eklenmiş formlara bağlanabilen eklenmiş formlarla tanımlanmaktadır.

Bir formun elemanları ses, ve (her biri sesli ve sessiz) resim, grafik, metin; ve matris, tablo, ajanda, para, metin, tarih, (her biri sesli ve sessiz) canlandırılmış resim ve grafik; alt-sınıf, eklenmiş form, kodlanmış değer, ve diğerleri, bir menüden seçilebilen ve her biri yukarıdaki türlerden biri olabilen değişken türler olabilir.

Sistemin modeli ilişkisel olmamakla birlikte, ilişkisel model tasarlanan modelin özel bir biçimidir.

Sistemin anlatım gücü, diğerlerinin yanında, mühendislik, büro, ve eğitim sistemleri gibi gerçek yaşamda karşılaşılan bilgi sistemlerinin çok yaklaşık modellerini tasarlamaya yeterlidir.

Kullanıcı etkileşimi sadece form doldurmak, menu ve listelerden seçim yapmak aracılığı ile sürdürülmektedir.

En önemli parçaların hepsi gerçekleştirilmiş ve bunlara dayalı olarak diğer parçaların tamamlanması çalışmaları gelecektede sürdürülecektir.

Anahtar Sözcükler : Veri tabanı yönetim sistemi,
bilgi yönetim sistemi.

A MULTI-MEDIA INFORMATION MANAGEMENT SYSTEM

Mehmet Erol Sanliturk

The data base technology between the years 1970 and 1995, has made very important contributions to the society and matured considerably as data base types of hierarchical, network, and especially relational. With the advancements in the hardware part, new ideas have also emerged in the data base area such as object-oriented, expert, multi-media data base systems, and knowledge systems.

The system that will be presented manages an information base by using at least three separate data bases : An application data base, a definition data base of the application data base, and a data base for management of users and their privileges on the application data base. Although it is not mandatory, if rules are to be used for the application data base, it is necessary to define rules within a rule data base to be used for inferences on application data base. Another important feature of the system is that definition of data base, users base and rule base are also data bases manageable by the system itself.

The main elements of the data bases are objects within classes in which objects will have inference capability with procedural computations and multi-media elements and there may be many classes within a data base. Each object is defined by a main form and member forms attacheable to main and member forms.

Elements of a form may be voice, and picture, graphics, text (each with or without voice), matrix, spreadsheet, agenda, money, text, date, animated picture and graphics (each with or without voice), sub-class, an attached form, coded entity, others, and a menu of variant elements each of which may be one of the types specified above.

The model of the system is object-oriented with complex objects, but not relational, however the relational model is a special case of it.

The expressive power of the system is sufficient to design very approximate models of real life information systems such as engineering, office, and educational systems among others.

The user interaction is only through form filling, and selection from menus and lists.

Implementation of all of the critical parts are completed, and work is continuing towards the completion of other parts based on the completed parts.

Key words : Data base management system, information management system, knowledge base management system.